Competition between Tetrahedral and Octahedral Symmetries in ^{152}Sm Nucleus:

A new set of data from a dedicated experiment

Tumpa Bhattacharjee,

Variable Energy Cyclotron Centre, Kolkata, India

We are Here

Arctic Ocean
OnTheWorldMap.com
France
Atlantic Ocean
Pacific Ocean
VECC, India
Indian Ocean
Pacific Ocean
Atlantic Ocean
Southern Ocean
Copyright © Ontheworldmap.com

We are Here

Variable Energy Cyclotron Centre

Homi Bhabha National Institute

The institute and City of Cyclotrons

K-130 (E ~ 7 – 10 MeV/u)

$^{14}N^{4+}$, $^{16}O^{5+}$, $^{20}Ne^{6+}$, $^{32}S^{10+}$, …..etc.

^{1}H, ^{2}H, ^{4}He

- High energy Light ion beam

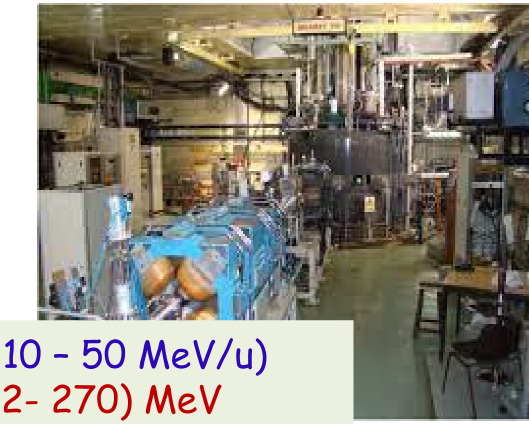

K-500 (E ~ 10 – 50 MeV/u)

$^{14}N^{4+}$ (252- 270) MeV

$^{16}O^{5+}$ (330 – 362) MeV,

$^{20}Ne^{6+}$ (397 – 434) MeV

30 MeV H Cyclotron

- Adjustable from 15- 30 MeV
- I ~ 350 μA

^{18}F (produce FDG for PET)

^{67}Ga, ^{201}Tl, ^{123}I (SPECT)

E ~ 415 keV (N^{4+})

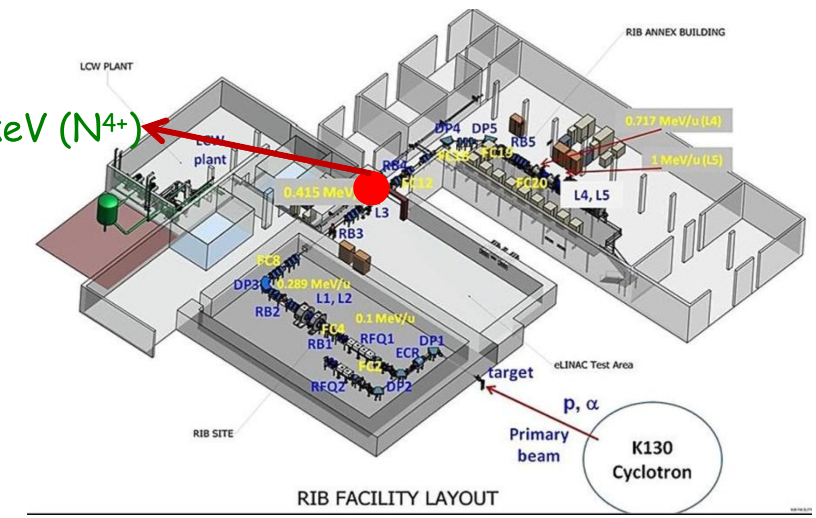

RIB (E ~ 100keV/u, I~ 8000 p/sec)

^{11}C, ^{11}CO, $^{11}CO_2$, ^{14}O, ^{43}K, ^{41}Ar

Instruments for Nuclear Physics Experiment

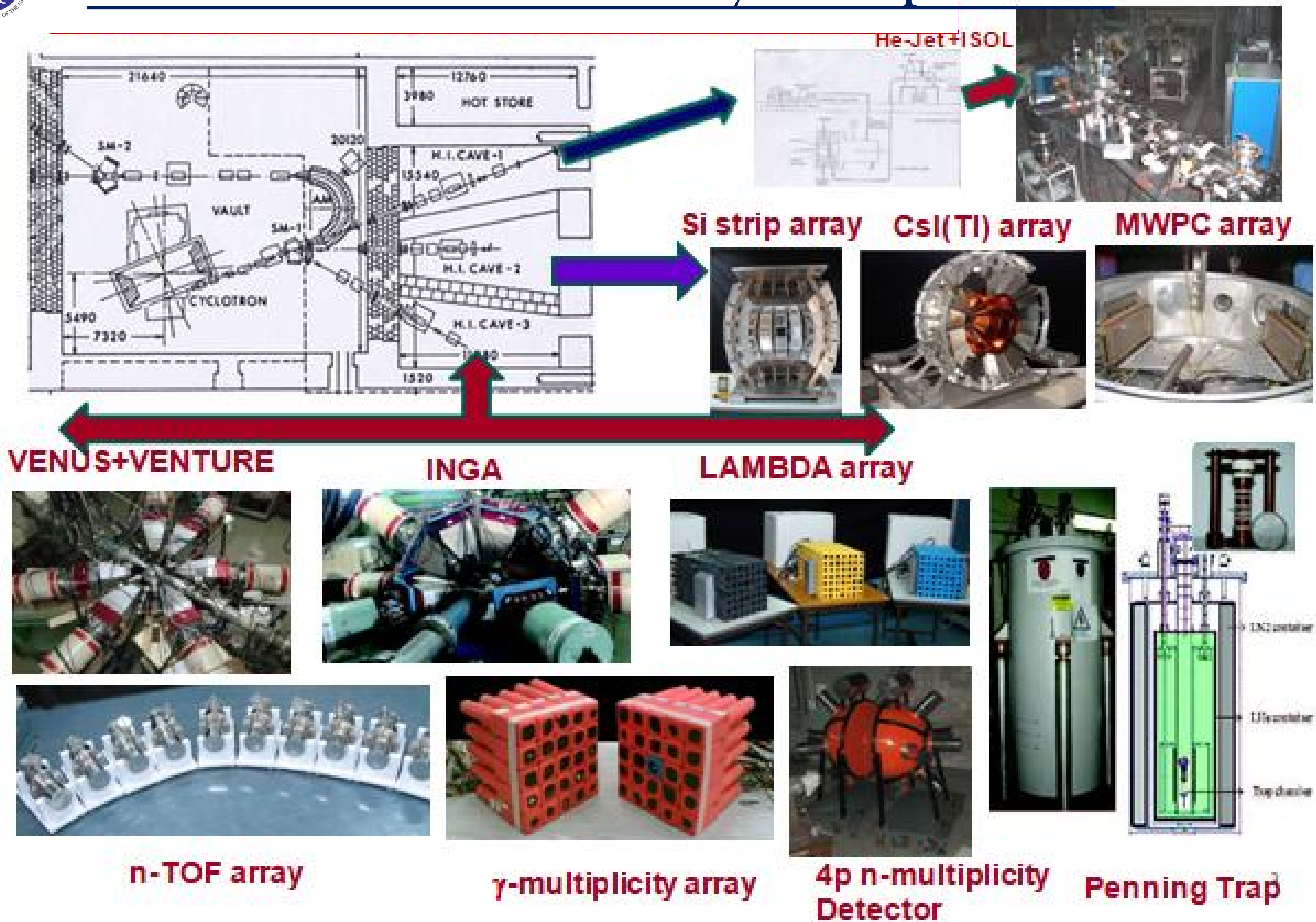

Setup for high resolution γ-ray Spectroscopy

A. Saha et al., Nucl. Phys. **A 976**, 1 (2018)

Soumik Bhattacharya et al., Phys. Rev. C **98**, 044311 (2018)

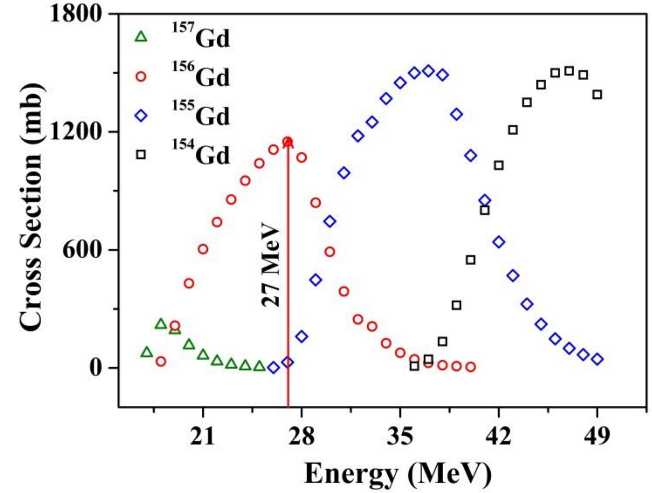

VECC array for **NU**clear **S**pectroscopy
EIGHT Compton suppressed Clover HPGe detectors

Spectroscopy with light ion beam

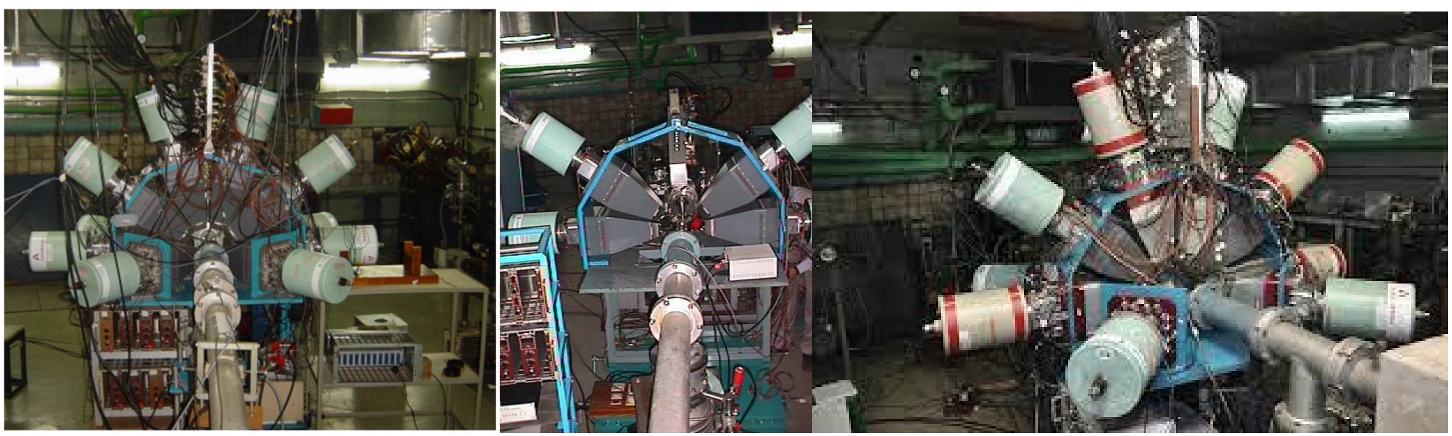

Indian National Gamma Array (INGA)
Compton suppressed Clover HPGe detectors – pulled from many institutes

Setups for γ–γ fast timing Spectroscopy

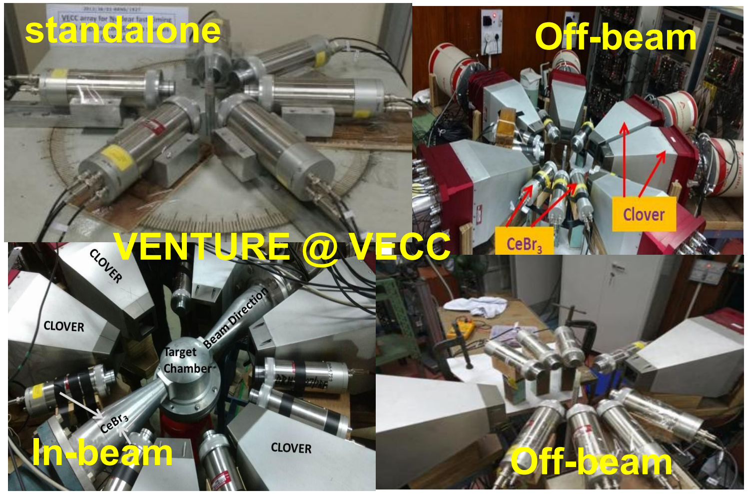

VECC array for **N**uclear fast **T**iming and ang**U**lar Cor**RE**lation studies **(VENTURE)**

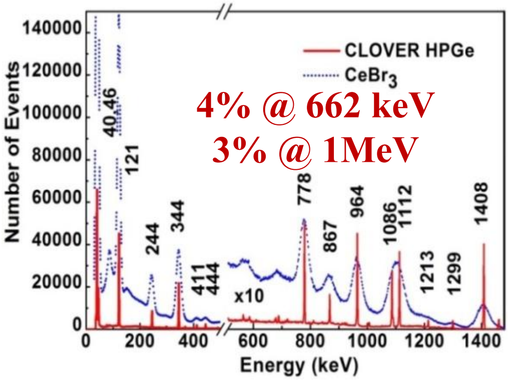

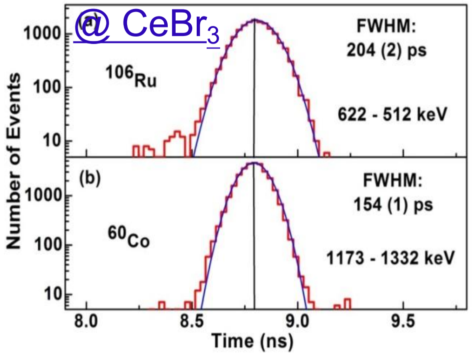

1. *S. S. Alam, TB, et al.*, NIM Phys. Res. **A 874** 103 (2017)
2. S. S. Alam, TB,,,,,Phys. Rev. C 99, 014306 (2019) .
3. S. Basak,....TB, Phys. Rev. **C 104**, 024320 (2021).
4. S. S. Alam, D. Banerjee, TB et al., Eur. Phys. Jour. A **56**, 269 (2020).

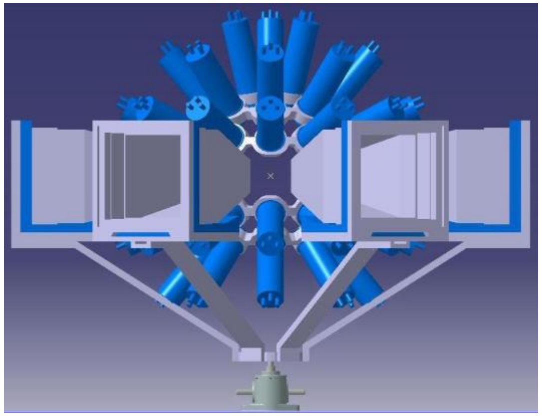

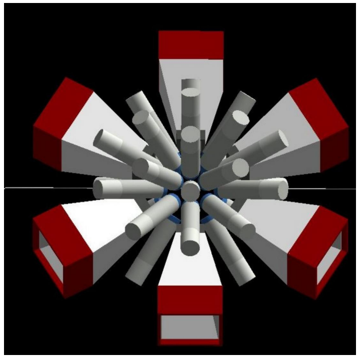

Recent measurement
Lifetimes in ^{154}Gd

Poster at SSNET 2024

VENTURE - 2.0 with 2in. x 1 in. LaBr/CeBr

Setups for γ–γ fast timing Spectroscopy

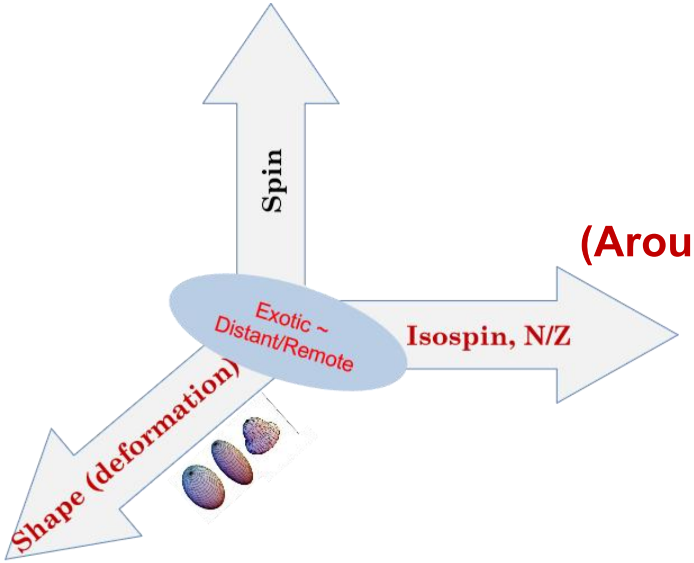

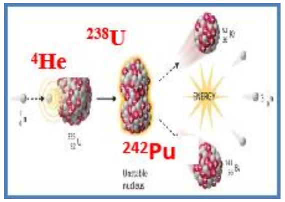

Radiochemical separation at VECC
OR
LOHENGRIN at ILL

(Around Z = 50, N = 82)

^{130}Xe	^{131}Xe (stable)	^{132}Xe (stable)	^{133}Xe (5d)	^{134}Xe (stable)	^{135}Xe (9h) N/Z=1.5	^{136}Xe (stable)	^{137}Xe	54
^{129}I	^{130}I	^{131}I (8d)	^{132}I (2h)	^{133}I (21h)	^{134}I (53h)	^{135}I (6.6h)	^{136}I	53
^{128}Te	^{129}Te	^{130}Te (stable)	^{131}Te (33h)	^{132}Te (3.2d)	^{133}Te (55m)	^{134}Te (42m)	^{135}Te	52
^{127}Sb	^{128}Sb	^{129}Sb	^{130}Sb (40m)	^{131}Sb	^{132}Sb (4 min)	^{133}Sb	^{134}Sb	51
^{126}Sn	^{127}Sn	^{128}Sn	^{129}Sn (2 min)	^{130}Sn	^{131}Sn	^{132}Sn N/Z=1.6	^{133}Sn	50
76	77	78	79	80	81	82	83	

Z →

N →

(Around Z = 64, N = 90 & Z = 40, N = 60)
Measurement of lifetime to determine E0 rates

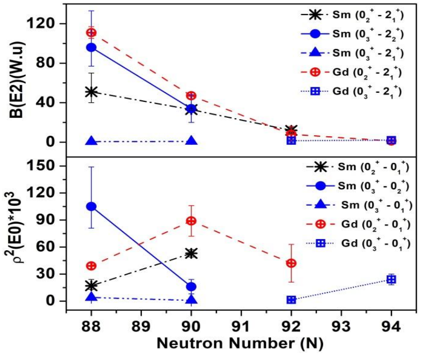

S. Basak, S. S. Alam, D. Kumar, A. Saha, D. Banerjee and TB Phys. Rev. C **104**, 024320 (2021).

D. Kumar, TB et al., Phys. Rev. C **106**, 034306 (2022)

D. Kumar, ...TB et al., Phys. Rev. C **109**, 024304 (2024)

Deformed Nuclei – Rotational Symmetry breaking

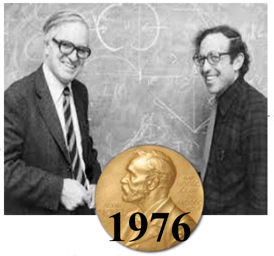

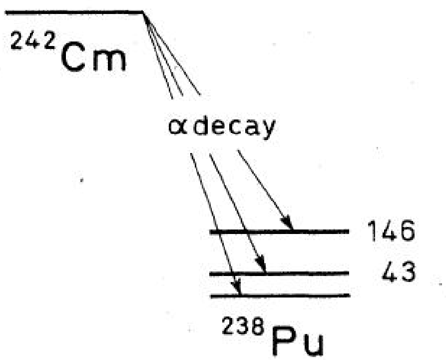

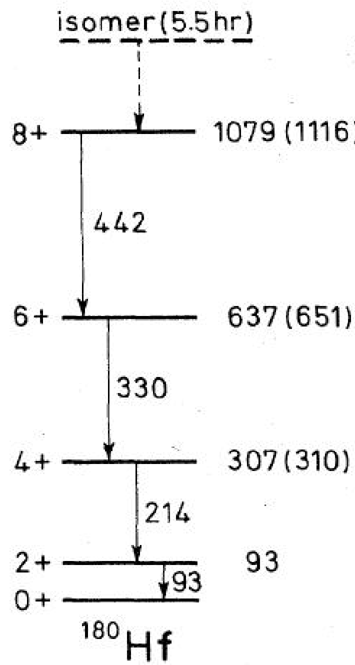

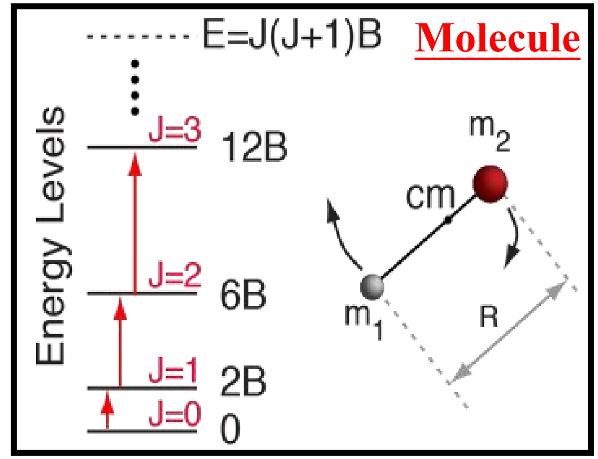

Collective excitation

$$E = \left(\frac{h}{2\Im}\right) . J\,(J+1)$$

Aage Bohr and Ben R. Mottelson, Phys. Rev. 89, 316 (1953); Phys. Rev. **90**, 717 (1953).

Reviews of Modern Physic, Vol. 48, No. 3, July 1976

All nuclei are not spherical!! Some are like Cigar or Disc!!

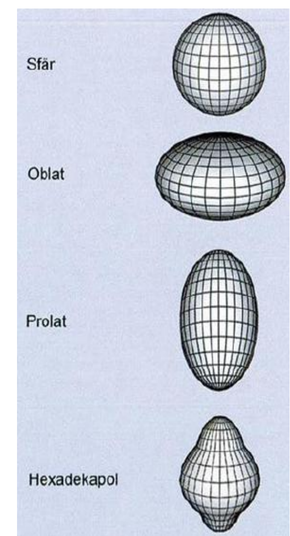

Shapes of Atomic Nuclei

$$R(\theta,\varphi) = R_0[1 + \Sigma_\lambda \Sigma_\mu \alpha_{\lambda\mu} Y_{\lambda\mu}(\theta,\varphi)]$$

R_0 = radius of a sphere

$\alpha_{\lambda\mu}$ = coefficients represent distortions from the equilibrium spherical shape

$\lambda=0$
Sphere

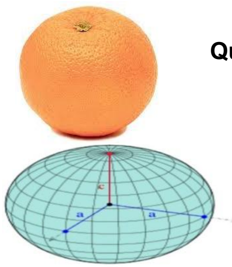

Oblate

λ=2, μ=0
Quadrupole Shape

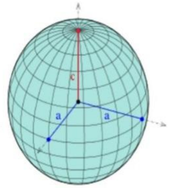

Prolate

λ=2, μ=±2
Triaxial Shape

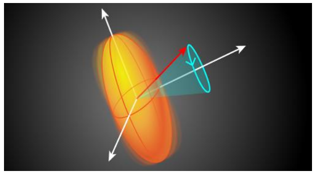

λ=3, μ=0
Octupole Shape

λ=3, μ=2
Tetrahedral Shape

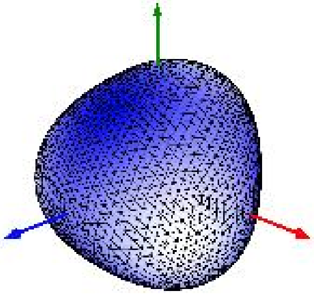

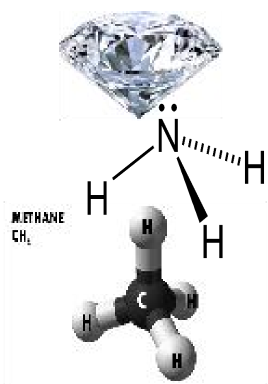

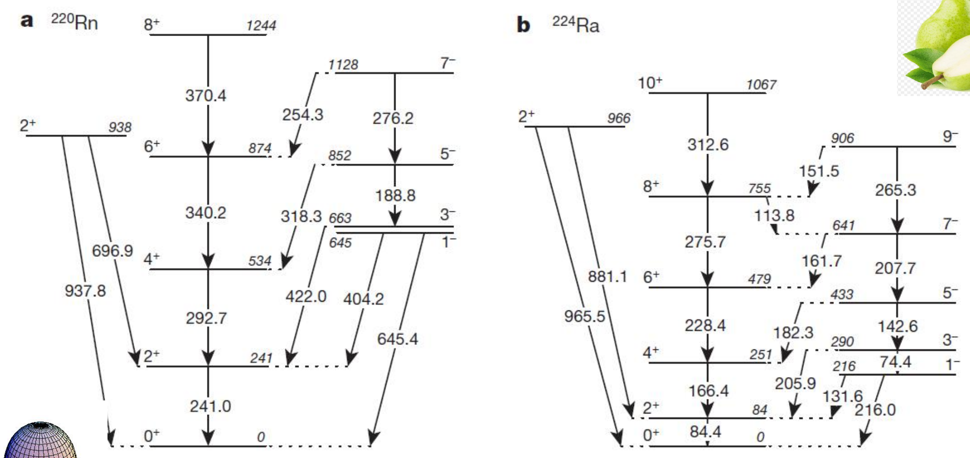

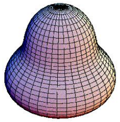

L. P. Gaffney et al., Nature ***497,*** *199 (2013)*

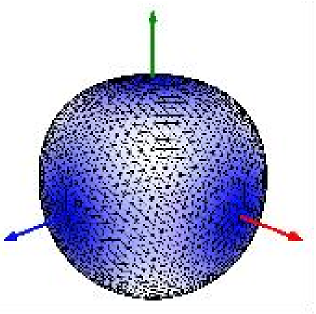

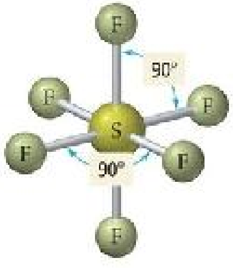

λ=4, μ=0
Otahedral Shape

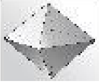

Nuclear Shell Gaps – Spherical & Deformed Nuclei

$$\mathcal{H} = \frac{P^2}{2m} + \frac{1}{2}m[\omega_\perp^2(x^2+y^2)+\omega_z^2 z^2] + C\vec{l}\cdot\vec{s} + D\vec{l}\cdot\vec{l}$$

Binding states of individual nucleons in strongly deformed nuclei

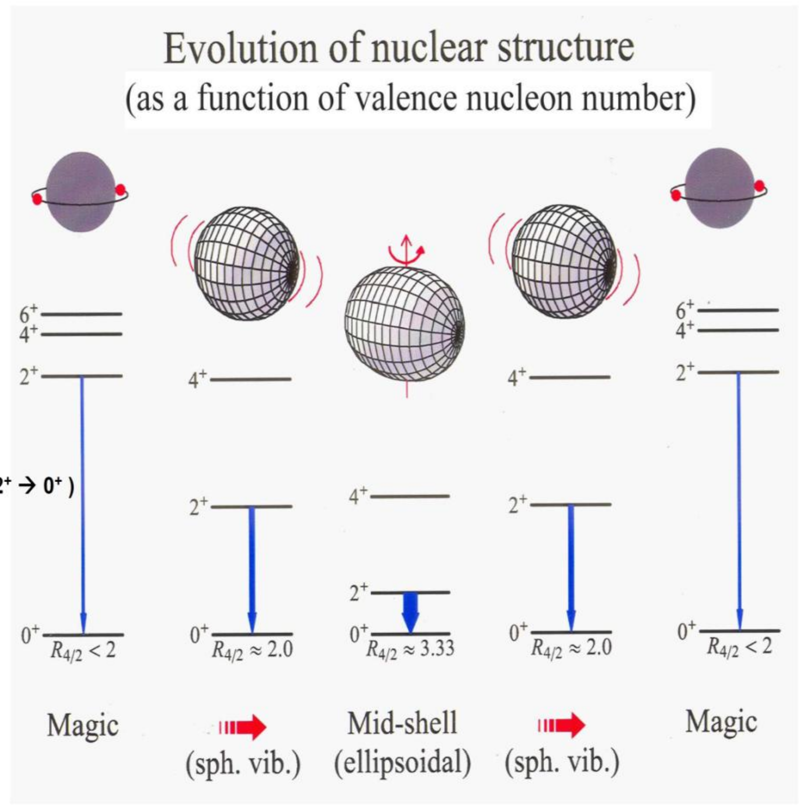

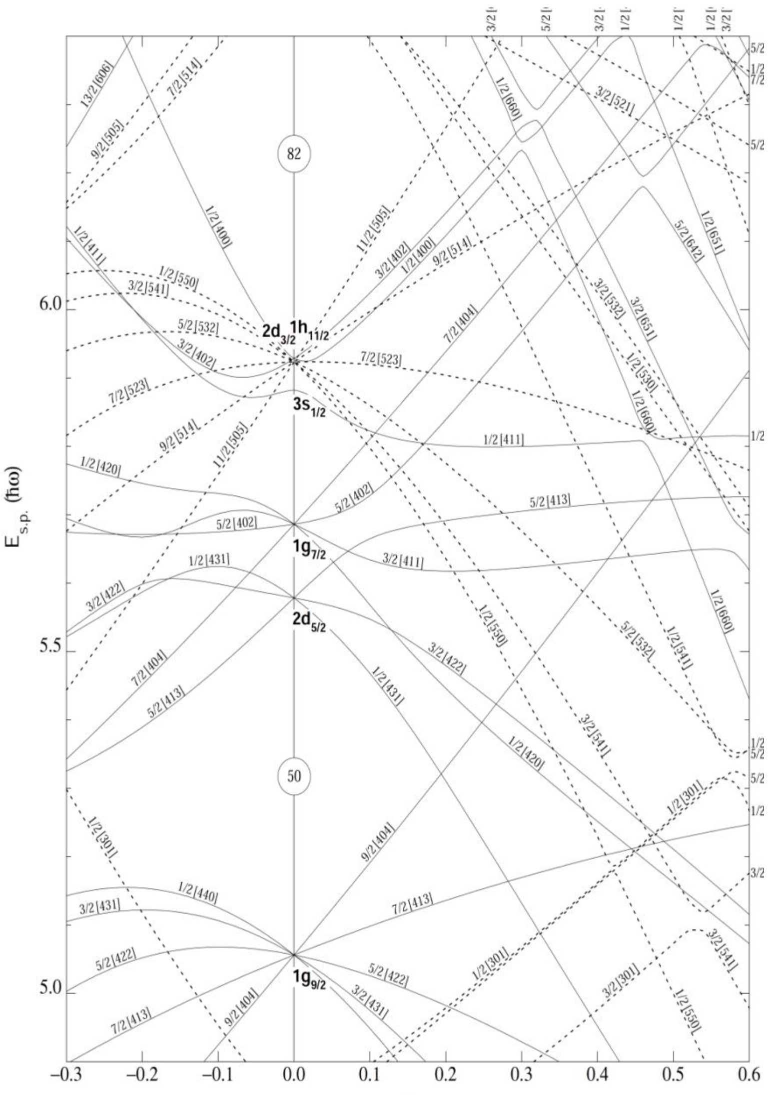

S. G. Nilsson, Kgl. Danske Videnskab. Selskab, Mat.-fys.Medd. **29**, No.16 (1955).

Tetrahedral Symmetry breaking ($\alpha_{32} \neq 0$)

$$\Sigma: \quad R(\vartheta,\varphi) = R_0\, c(\{\alpha\}) \left[1 + \sum_{\lambda} \sum_{\mu} \alpha^{*}_{\lambda\mu} Y_{\lambda\mu}(\vartheta,\varphi) \right]$$

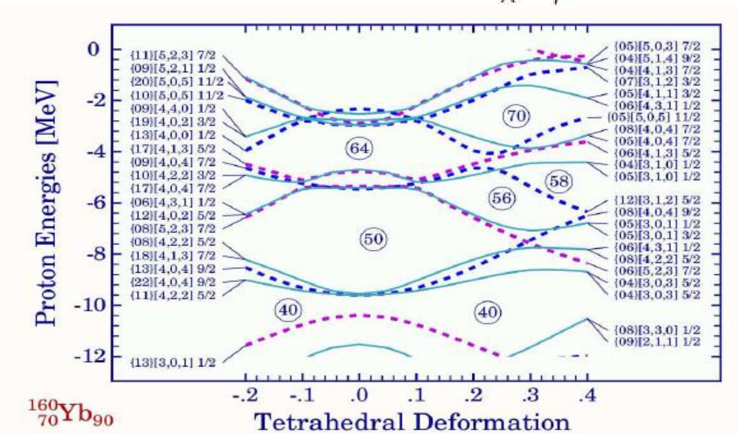

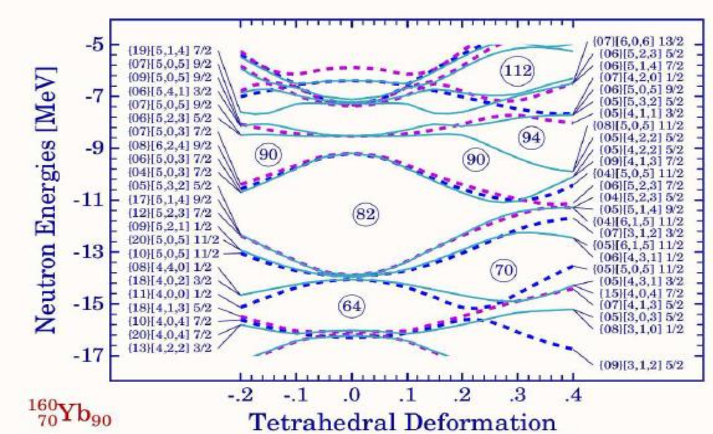

Phys. Rev. Lett. 88, 252502 (2002),
Phys. Rev. Lett. 97, 072501 (2006)

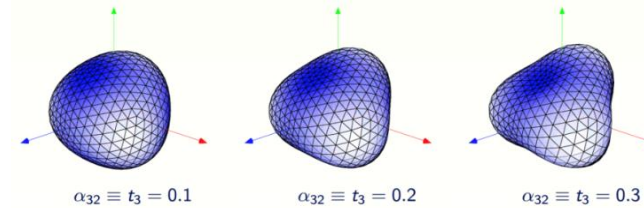

No.	Group	No. Irr.	No.×Dimensions
01.	O_h^D	6	4 x 2D and 2 x 4D
02.	O^D	3	2 x 2D and 1 x 4D
03.	T_d^D	3	2 x 2D and 1 x 4D
04.	C_{6h}^D	12→ 6	12 x 1D
05.	D_{6h}^D	6	6 x 2D
06.	T_h^D	6	6 x 2D
07.	D_{4h}^D	4	4 x 2D
–	D_{2h}^D	2	2 x 2D (reference)

$T_d^{\,D}$ → Tetrahedral double point group (48 symmetry elements)

2 families of 2 fold degenerate energy levels,
1 family of 4 fold degenerate energy levels

Higher fold degeneracies of nucleonic levels

→ Exotic symmetry breaking in nuclei

Tetrahedral Symmetry breaking ($\alpha_{32} \neq 0$)

Evidence of tetrahedral shape in Nuclei :
Cluster state in ^{16}O (Light nuclei)

PRL 112, 152501 (2014)

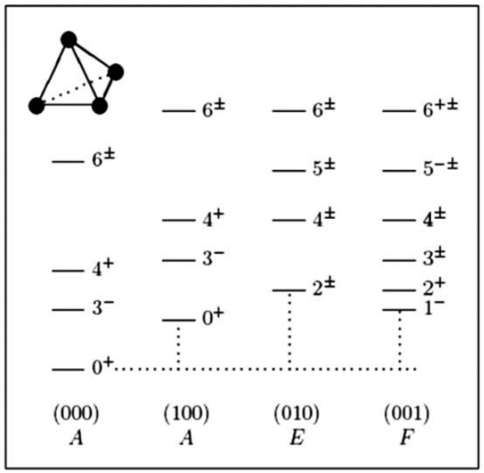

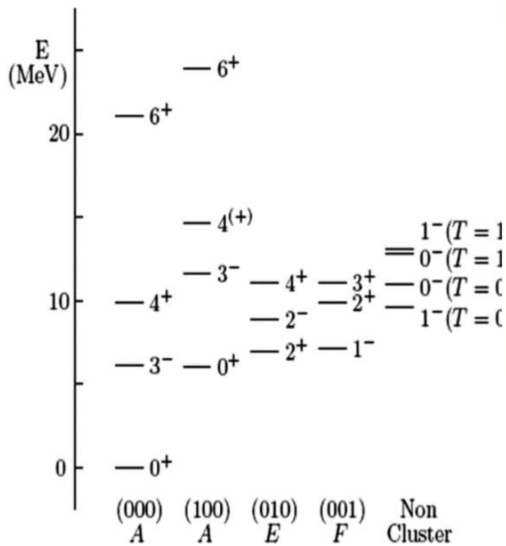

Theory
(Algebric Cluster Model)

Experiment

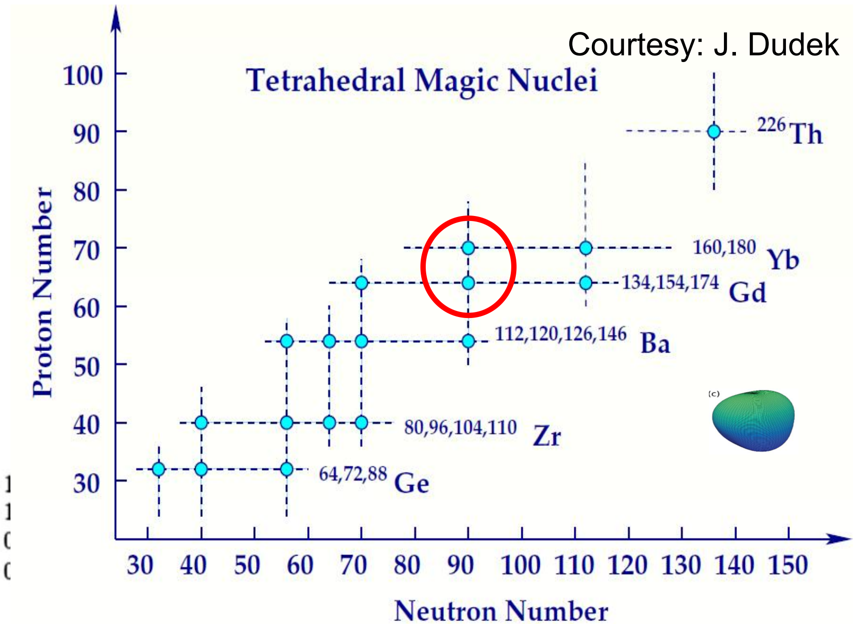

Z/N→16, 20, 32, 40, 56, 64, 70, 90
N → 112, 136, 142
(Tetrahedral Magic Gaps)

Tetrahedral Symmetry breaking ($\alpha_{32} \neq 0$)

TABLE VI. The number of states $a_i^{(I\pi)}$ belonging to the five irreducible representations of T_d for integer spins; those for each parity are separately shown.

I^+	0^+	1^+	2^+	3^+	4^+	5^+	6^+	7^+	8^+	9^+	10^+	11^+	12^+	13^+	14^+	15^+	16^+
A_1	1	0	0	0	1	0	1	0	1	1	1	0	2	1	1	1	2
A_2	0	0	0	1	0	0	1	1	0	1	1	1	1	1	1	2	1
E	0	0	1	0	1	1	1	1	2	1	2	2	2	2	3	2	3
$F_1(T_1)$	0	1	0	1	1	2	1	2	2	3	2	3	3	4	3	4	4
$F_2(T_2)$	0	0	1	1	1	1	2	2	2	2	3	3	3	3	4	4	4
I^-	0^-	1^-	2^-	3^-	4^-	5^-	6^-	7^-	8^-	9^-	10^-	11^-	12^-	13^-	14^-	15^-	16^-
A_1	0	0	0	1	0	0	1	1	0	1	1	1	1	1	1	2	1
A_2	1	0	0	0	1	0	1	0	1	1	1	0	2	1	1	1	2
E	0	0	1	0	1	1	1	1	2	1	2	2	2	2	3	2	3
$F_1(T_1)$	0	0	1	1	1	1	2	2	2	2	3	3	3	3	4	4	4
$F_2(T_2)$	0	1	0	1	1	2	1	2	2	3	2	3	3	4	3	4	4

Microscopic mean-field and residual-interaction Hamiltonians with angular-momentum and parity projection method

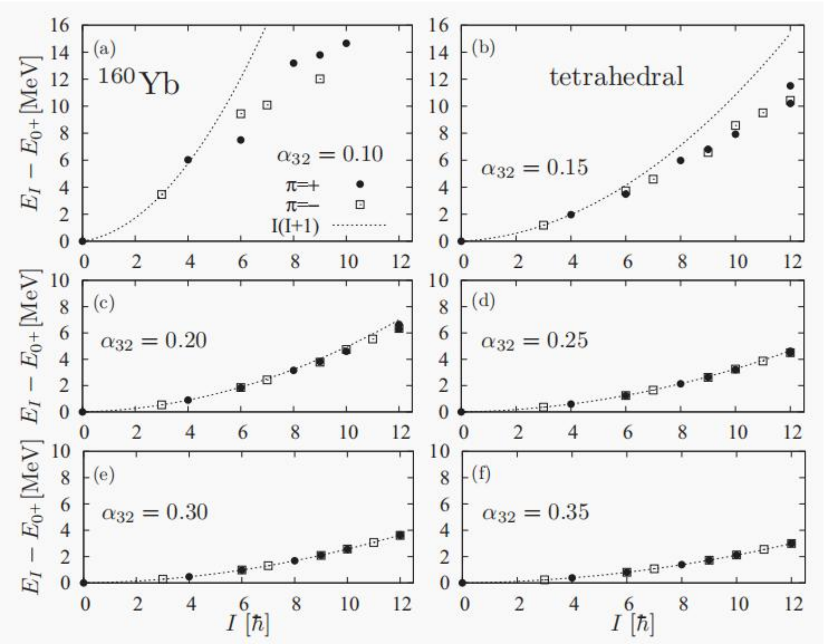

S. Tagami et al., PRC **87**, 054306 (2013)

Lowest Irrep for T_d symmetry

$A_1:\ I^\pi = 0^+, 3^-, 4^+, 6^\pm, 7^-, 8^+, 9^\pm, 10^\pm, 11^-, \ldots$ → Exact T_d pattern

Two lowest irreps for O_h symmetry

$A_{1g}:\ 0^+, 4^+, 6^+, 8^+, 9^+, 10^+, \ldots,\ I^\pi = I^+,$ → Exact O_h, $I_\pi = 0^+$

$A_{2u}:\ 3^-, 6^-, 7^-, 9^-, 10^-, 11^-, \ldots,\ I^\pi = I^-,$ → Exact O_h, $I_\pi = 0^-$

→ Tetrahedral double point group (T_d^D) is a subgroup of Octahedral double point group (O_h^D)

Tetrahedral Symmetry breaking ($\alpha_{32} \neq 0$)

Rotational band with E ~ I(I+1) → Bohr Theory

Lowest Irrep for T_d symmetry

$$A_1 : I^\pi = 0^+, 3^-, 4^+, 6^\pm, 7^-, 8^+, 9^\pm, 10^\pm, 11^-, \ldots$$

$$E_I \propto \frac{\hbar^2}{2\mathcal{J}_{T_d}} I(I+1)$$

Two lowest irreps for O_h symmetry

$$A_{1g} : \; 0^+, 4^+, 6^+, 8^+, 9^+, 10^+, \ldots, \; I^\pi = I^+,$$

$$E \propto \; = \frac{h^2}{2I_{A1g}} I\,(I+1)$$

$$A_{2u} : \; 3^-, 6^-, 7^-, 9^-, 10^-, 11^-, \ldots, I^\pi = I^-,$$

$$E \propto \; = \frac{h^2}{2I_{A2u}} I\,(I+1)$$

Pure tetrahedral structure

$$\mathcal{J}_{A_{1g}} \approx \mathcal{J}_{A_{2u}} \approx \mathcal{J}_{A_1}$$

Tetrahedral Symmetry breaking ($\alpha_{32} \neq 0$)

Courtesy: J. Dudek

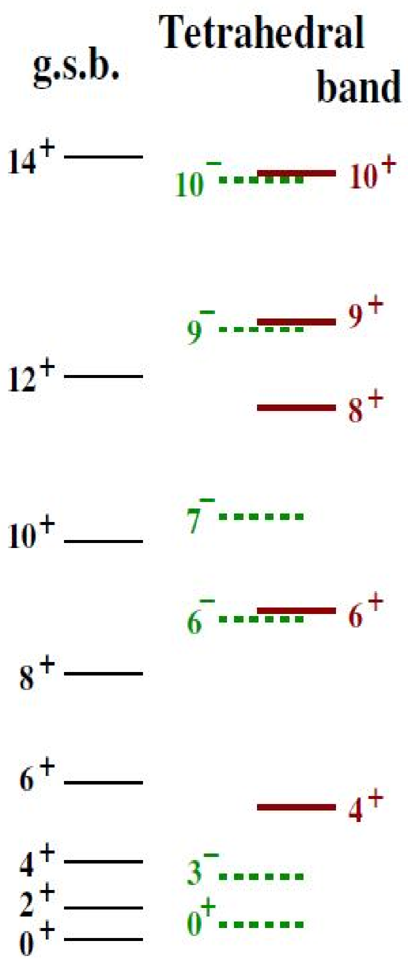

- For small deformations we may use Taylor expansion:

$$Q_{\lambda\mu}(\alpha) \approx Q_{\lambda\mu}\Big|_{\alpha=0} + Q'_{\lambda\mu}\Big|_{\alpha=0}\Delta\alpha + \frac{1}{2}Q''_{\lambda\mu}\Big|_{\alpha=0}\Delta\alpha\Delta\alpha$$

- We set $\lambda = 2$, $\mu = 0$ and $\lambda_1 = \lambda_2 = 3$, $\Delta\alpha \approx \alpha_{3\mu}\big|_{\alpha\ small} \rightarrow$

$$\alpha_{30}: \quad Q_{20} = 4/(3\sqrt{5\pi}) \cdot \alpha_{30}^2 \cdot \rho_0 R_0^5$$
$$\alpha_{31}: \quad Q_{20} = 6/(3\sqrt{5\pi}) \cdot \alpha_{3+1}\alpha_{3-1} \cdot \rho_0 R_0^5$$
$$\alpha_{32}: \quad Q_{20} = 0 \leftarrow \text{Tetrahedral symmetry}$$
$$\alpha_{33}: \quad Q_{20} = 10/(3\sqrt{5\pi}) \cdot \alpha_{3+3}\alpha_{3-3} \cdot \rho_0 R_0^5$$

E2 decay forbidden!!

E3 decay enhanced

B(E3) = ?? (order of magnitude)

$T(E1) = 1.59 * 10^{15} * E^3 B(E1)$

$T(E2) = 1.22 * 10^9 * E^5 B(E2)$

$T(E3) = 5.67 * 10^2 * E^7 B(E3)$

Existence of an isomeric band!!

Experimental identification becomes extremely challenging!!

Physics Interest in ^{152}Sm

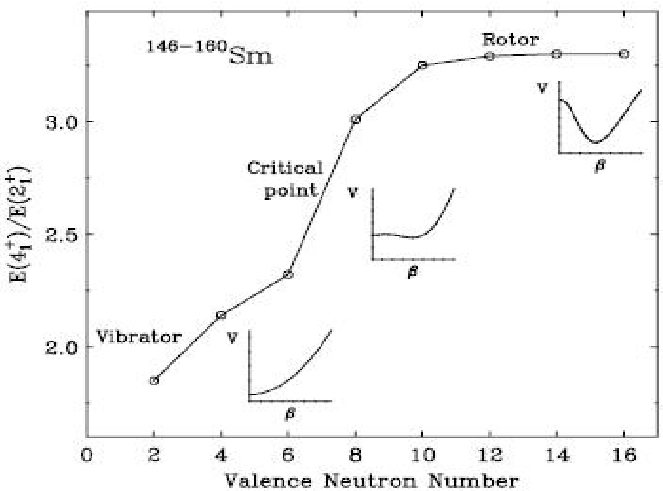

Phys. Rev. Lett. **87**, 052503 (2001)

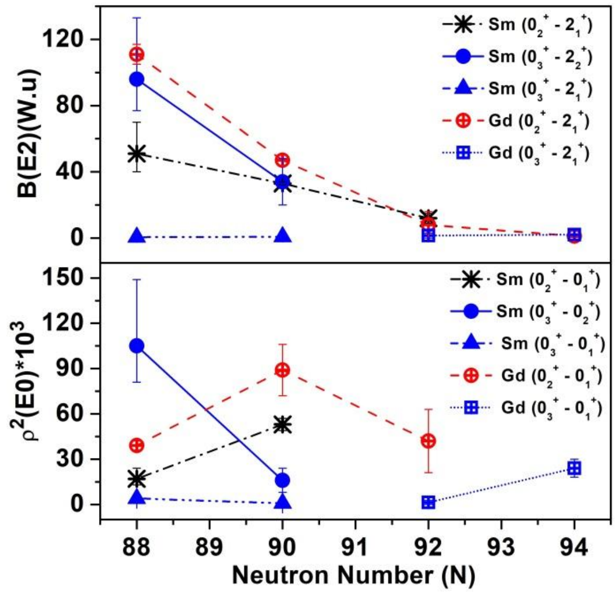

S. Basak, S. S. Alam, D. Kumar, A. Saha, D. Banerjee and TB Phys. Rev. C **104**, 024320 (2021).

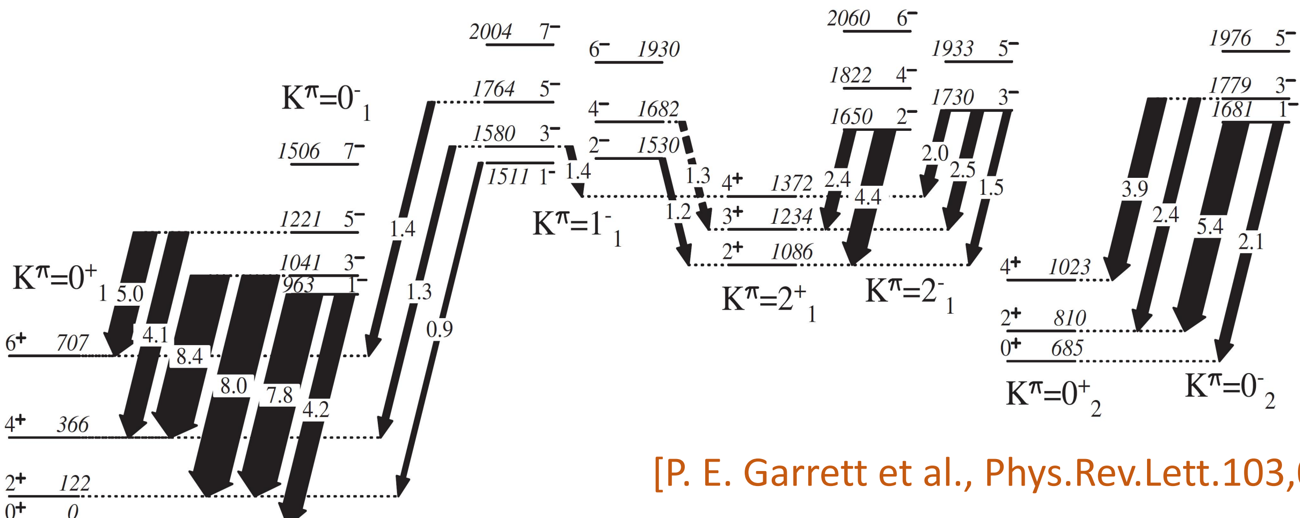

[P. E. Garrett et al., Phys.Rev.Lett.103,062501(2009)]

Physics Interest in ^{152}Sm

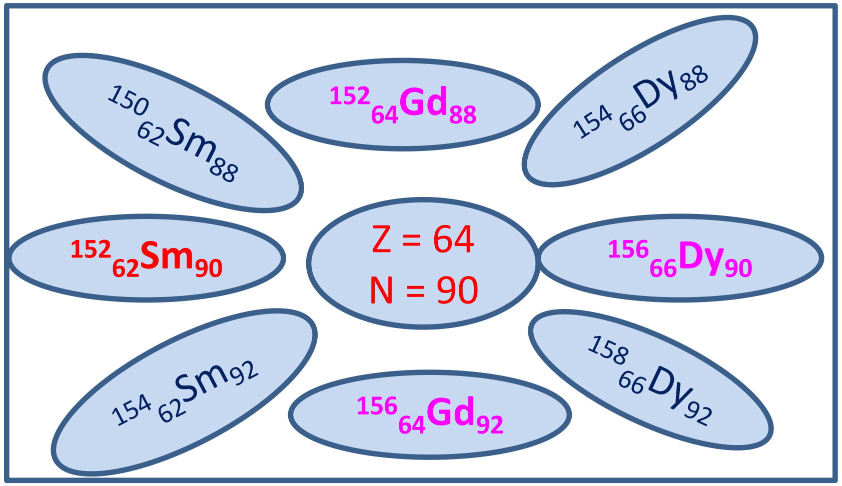

We are at Tetrahedral Magic Gap!!

Spin	E[keV]	No. D-out	No. Feed	Reaction
3^-	1579.4	10	none	CE & α
4^+	1757.0	9	1+(1)	CE & α
6^-	1929.9	2	(1)	CE & α
6^+	2040.1	7	none	CE & α
7^-	2057.5	6	2+(1)	CE & α
8^+	2391.7	3	1	CE & α
9^-	2388.8	4	3	CE & α
9^+	2588	2	1	α
10^-	2590.7	4	1	α
(10^+)	2810	2	none	α
11^-	2808.9	2	none	CE

J. Dudek et al., PRC 97, 021302(R) (2018)

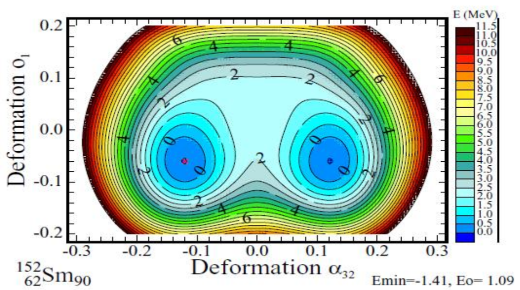

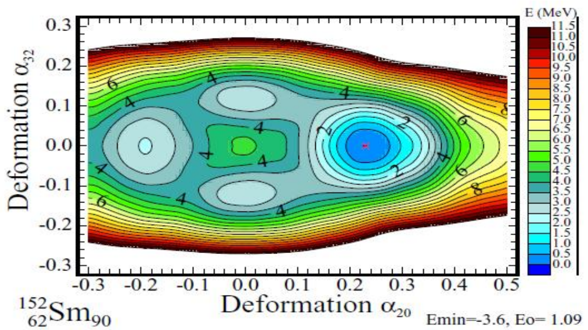

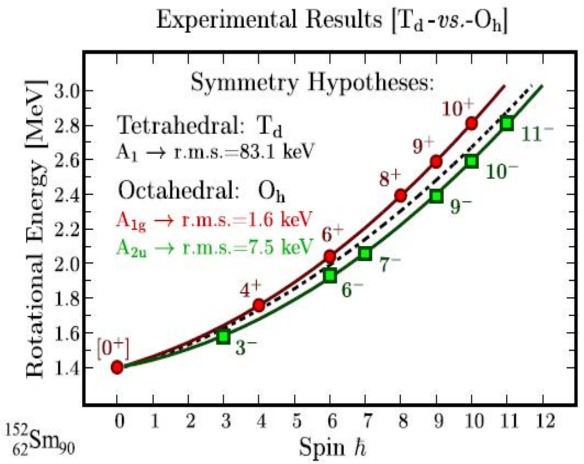

➢At vanishing quadrupole deformation, the minima in the PES is visible for non-zero a_{32}.

➢The energy of this minima decreases with the presence of non-zero octahedral deformation.

T_d(1) Band

Population of ^{152}Sm

- High statistics →

  High cross section

  Increased Target thickness

  High Beam current

  High efficiency Clover HPGe array

  Long beamtime

Keeping in mind: Limitation in Count rate in HPGe crystal 5- 6k/sec)

- Low angular momentum population
- Less contamination from neighboring evaporation channel

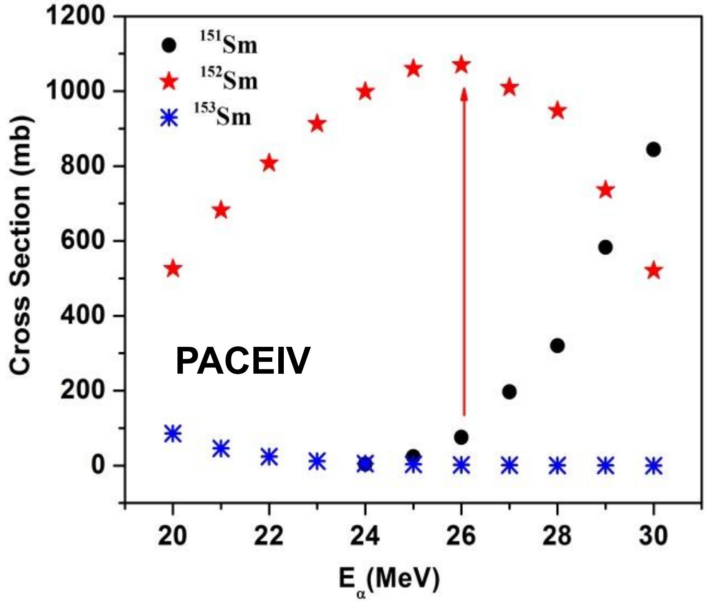

^{150}Nd (^{4}He, 2n) ^{152}Sm @ 26 MeV

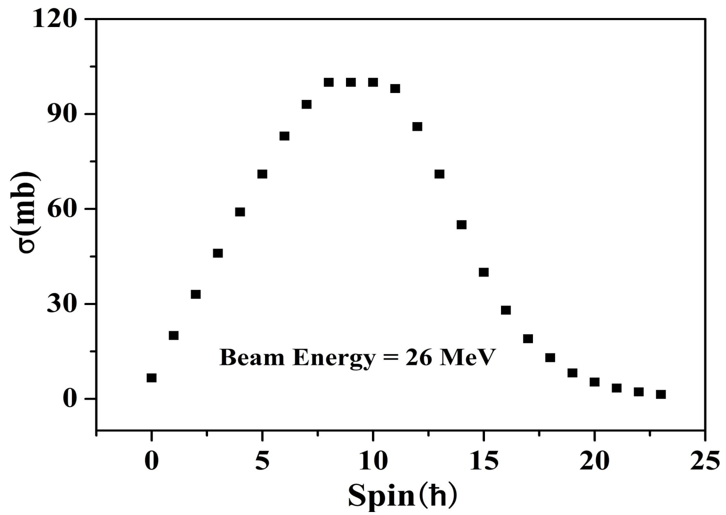

Gamma Array with local collaboration in Kolkata (VECC, SINP, UGC-DAE-CSR)

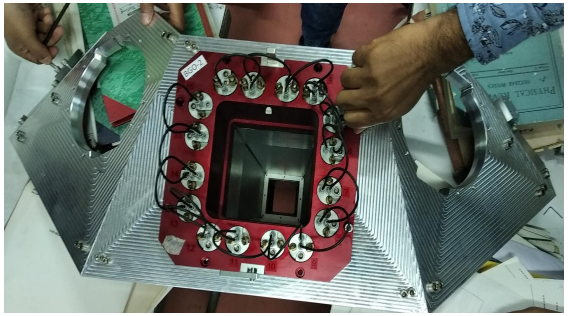

New segments MEG, VECC

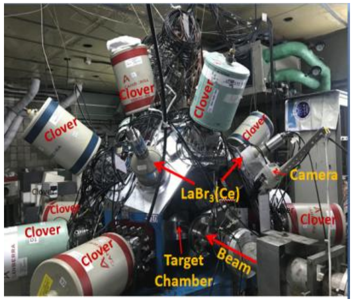

12 Detectors at:

90° : 6 Nos
40° : 3 Nos
125° : 3 Nos

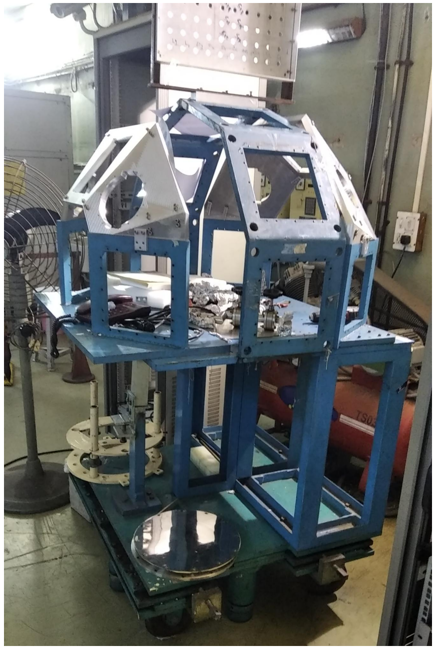

Comparison with existing experiment on ^{152}Sm

P. E. Garrett et al., J. Phys. G: Part & Nucl. Phys. 31, S1855 (2005)

- Performed with 9 single crystal HPGe and one Cluster HPGe detector
- Gathered 2 x 10^9 $\gamma-\gamma$ events, Used 1 x 10^9 $\gamma-\gamma$ events for the development of level scheme
- Beam energy : 22 MeV
- P/T ~ 0.28 (av)

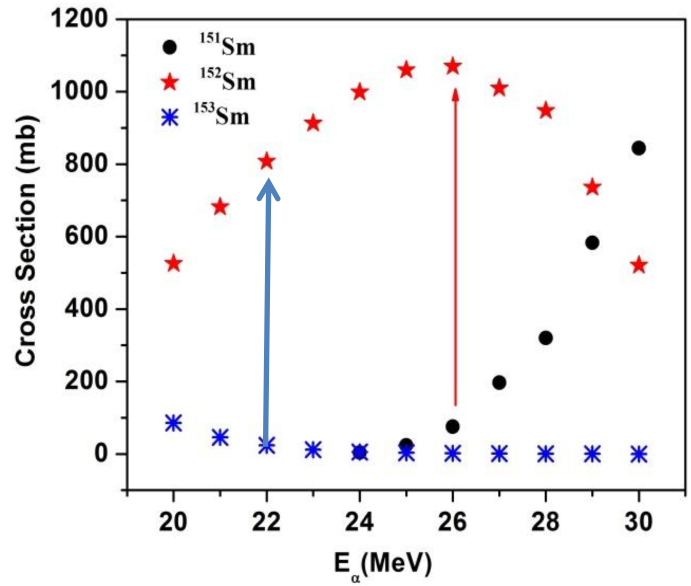

PRESENT EXPERIMENT:

- 12 Compton suppressed Clover HPGe detectors
- Beam Energy : 26 MeV
- $\gamma-\gamma$ statistics > 2 x 10^9
- P/T ~ 0.45

Gain

P/T ~ 1.6
Statistics ~ 2
1/sqrt(N) ~ 0.5

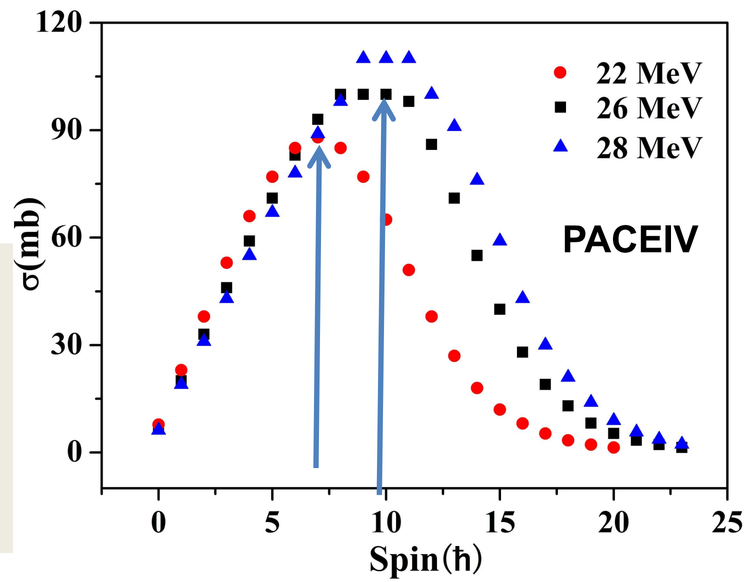

New candidate Tetrahedral sequence in ^{152}Sm

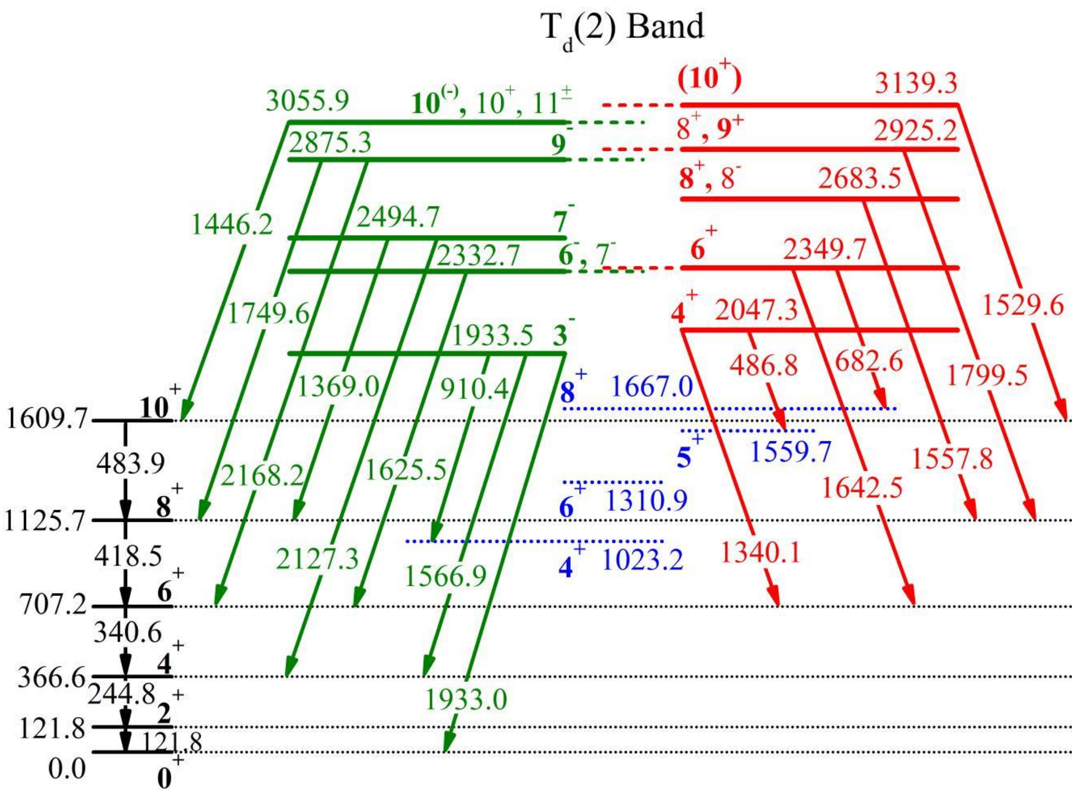

Beam current ~ 2.5nA

BOT ~ 11 days (effective)

Digital DAQ --> data written in Compton suppressed singles mode

Conventional γ- spectroscopy techniques

Measured

1. γ–γ & γ–γ–γ coincidences
2. Angular distribution a_2, a_4
3. Angular Correlation --> R_{DCO}
4. Linear Polarization P

Calculated

P vs R_{DCO} contours

P vs a_2 contours

New candidate Tetrahedral sequence in ^{152}Sm

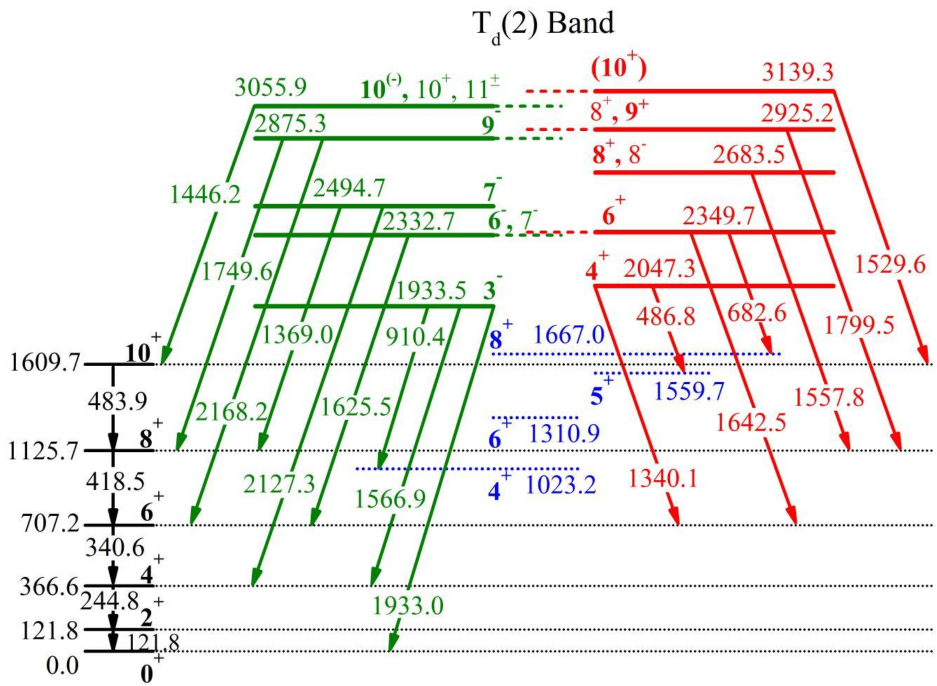

Relative Intensity

E_i (keV)	E_f (keV)	I_i^π	$\rightarrow I_f^\pi$	E_γ (keV)	I_γ
1933.5(8)	1023.22(4)	3^-	$\rightarrow 4^+$	910.4(1)	0.20(2)
	366.60(2)		$\rightarrow 4^+$	1566.9(2)	0.18(2)
	0.0		$\rightarrow 0^+$	1933.0(8)	0.05(1)
2047.3(3)	1559.71(4)	4^+	$\rightarrow 5^+$	486.8(3)	0.71(13)
	707.21(4)		$\rightarrow 6^+$	1340.1(1)	0.77(6)
2332.7(2)	707.21(4)	6^-	$\rightarrow 6^+$	1625.5(1)	0.35(2)
2349.7(2)	1667.97(6)	6^+	$\rightarrow 8^+$	682.6(1)	0.14(2)
	707.21(4)		$\rightarrow 6^+$	1642.5(2)	0.12(1)
2494.7(4)	1125.75(6)	7^-	$\rightarrow 8^+$	1369.0(1)	0.10(1)
	366.60(2)		$\rightarrow 4^+$	2127.3(4)	0.07(1)
2683.5(2)	1125.75(6)	8^+	$\rightarrow 8^+$	1557.8(1)	0.46(2)
2875.3(5)	1125.75(6)	9^-	$\rightarrow 8^+$	1749.6(1)	0.15(1)
	707.21(4)		$\rightarrow 6^+$	2168.2(5)	0.05(1)
2925.2(2)	1125.75(6)	9^+	$\rightarrow 8^+$	1799.5(1)	0.27(2)
3055.9(2)	1609.69(7)	10^-	$\rightarrow 10^+$	1446.2(1)	0.14(2)
3139.3(2)	1609.69(7)	(10^+)	$\rightarrow 10^+$	1529.6(1)	0.17(3)

New candidate Tetrahedral sequence in ^{152}Sm

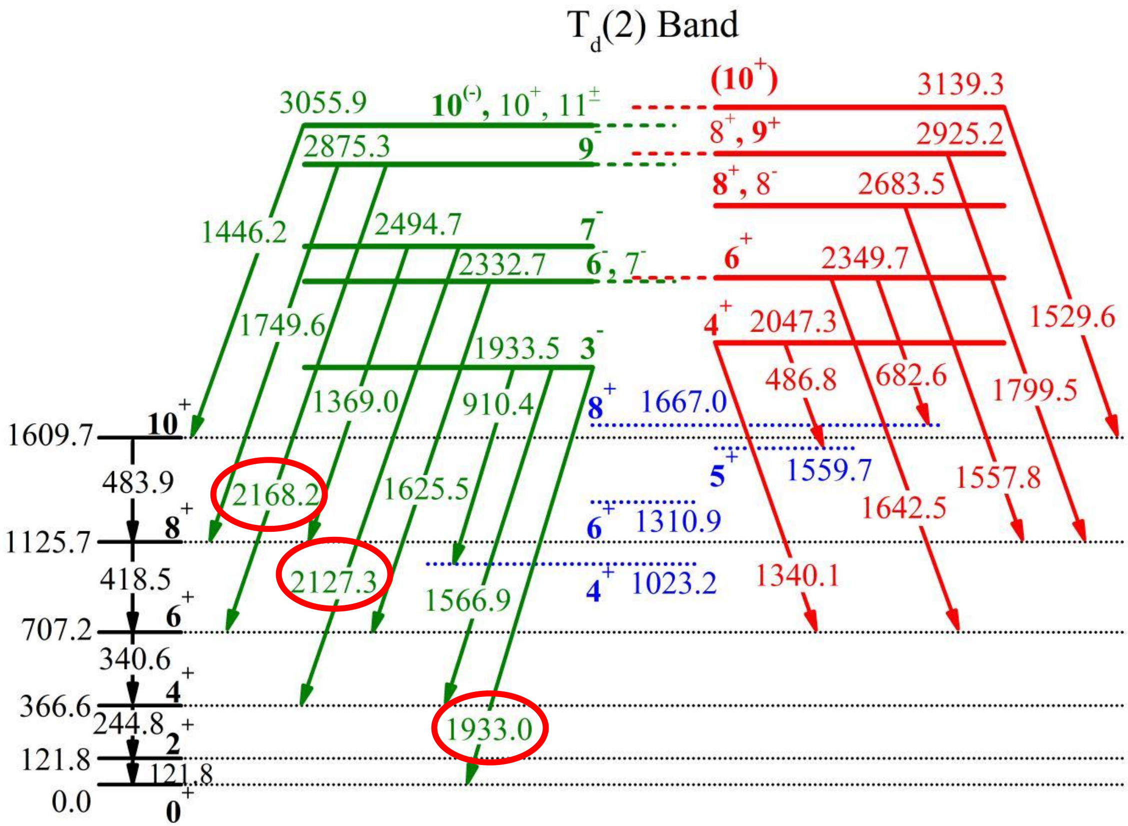

E3 Transitions

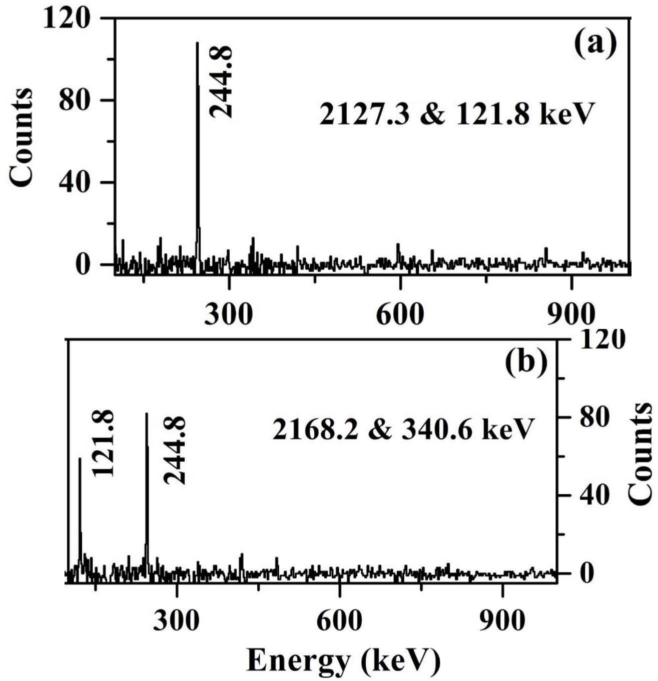

New candidate Tetrahedral sequence in ^{152}Sm

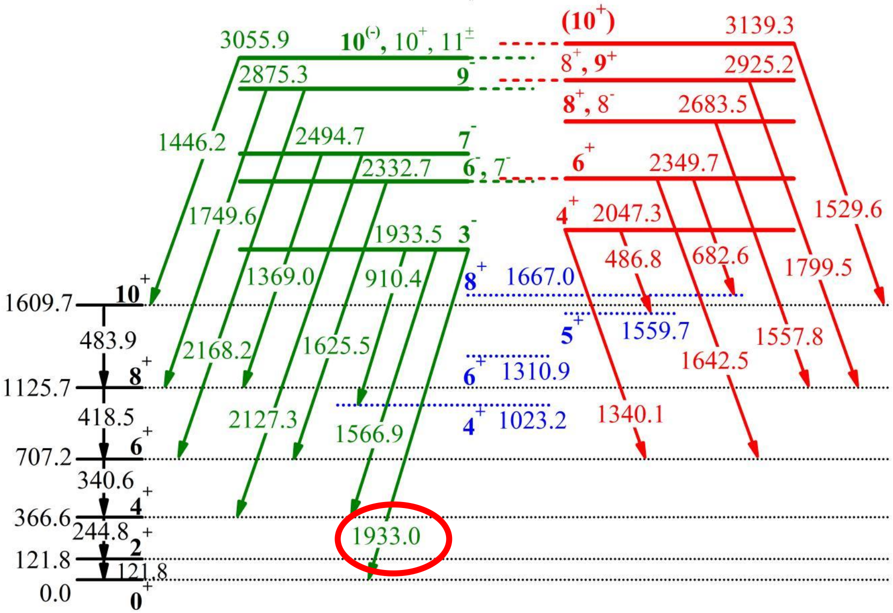

- Fitting singles projection at 90°, we observe a new transition with energy 1933.0(8) keV

- This 1933.0 keV is placed as $3^- \rightarrow 0^+$ decay

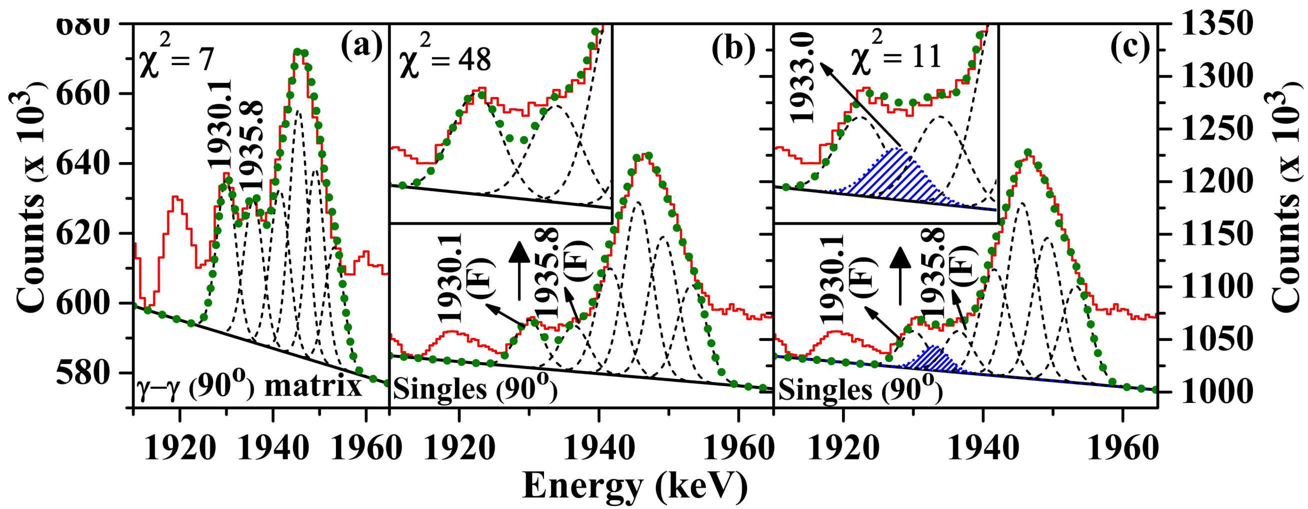

New candidate Tetrahedral sequence in ^{152}Sm

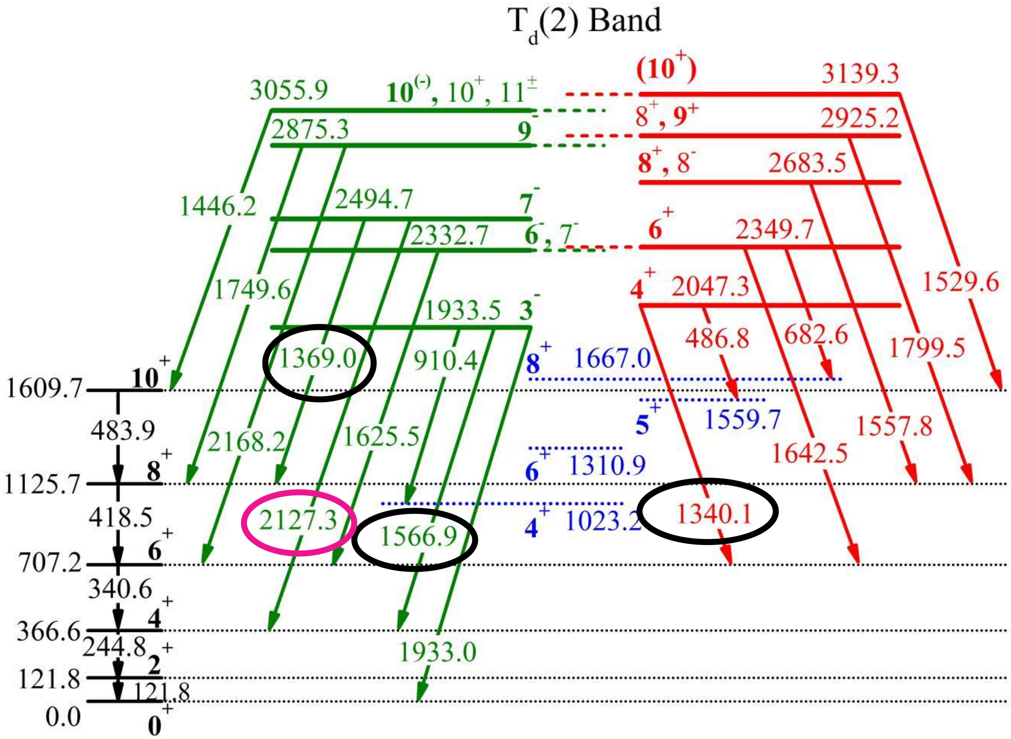

Zs Podolyak, C. M. Shand, E. Wilson, B. A. Brown H. Grawe, C. J. Chiara, S. Zhu, B. Fornal R V F. Janssens, *Jour. Phys. Conf. Ser.* **580**, 01201((2015).

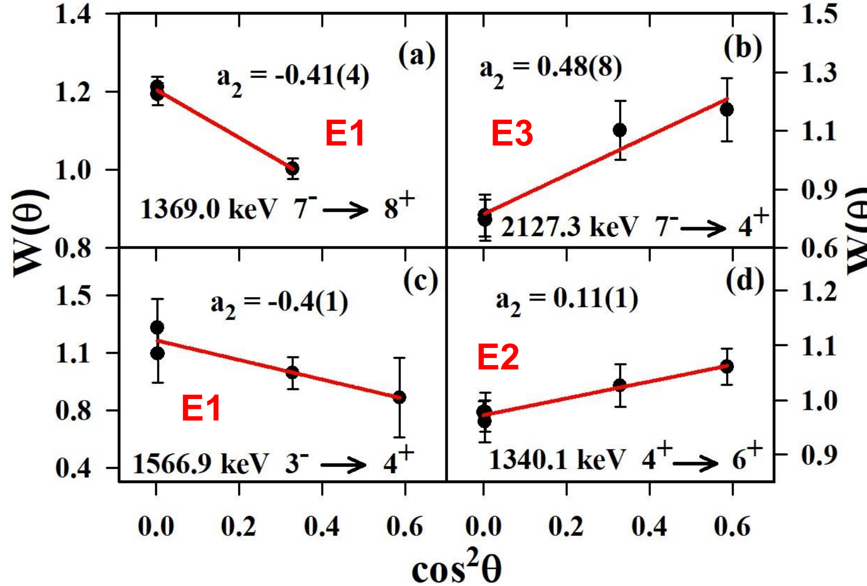

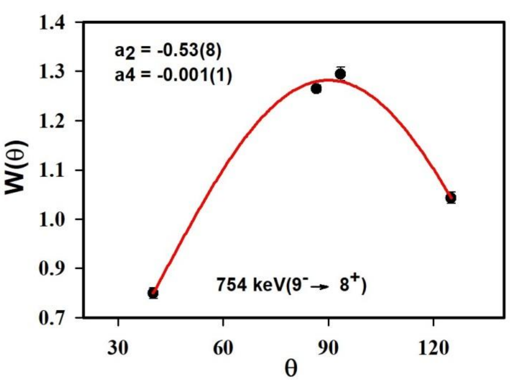

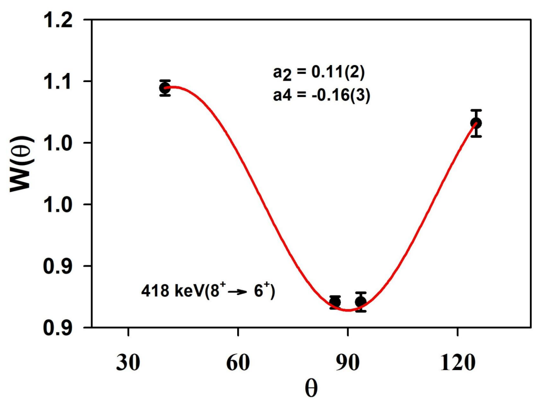

$a_2 = 0.55$ for the pure octupole transition of the $7^- \rightarrow 4^+$ decay

→ calculated from ANCORR code

New candidate Tetrahedral sequence in ^{152}Sm

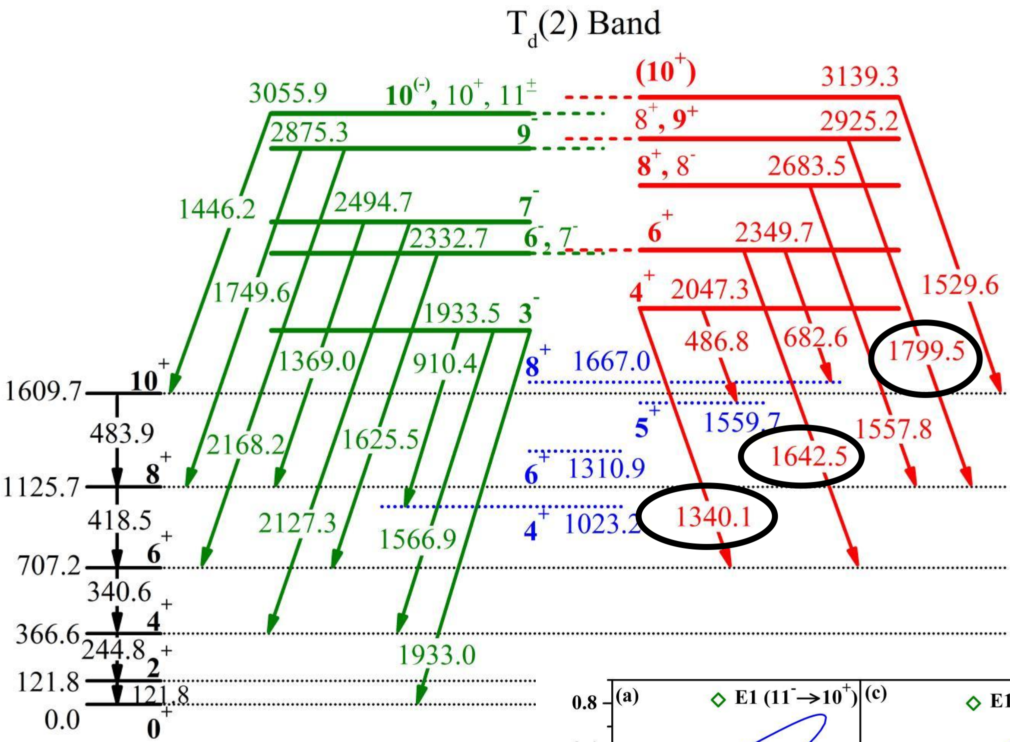

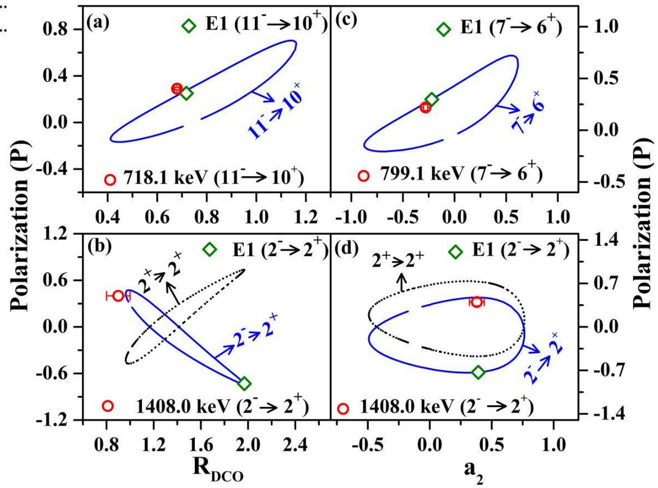

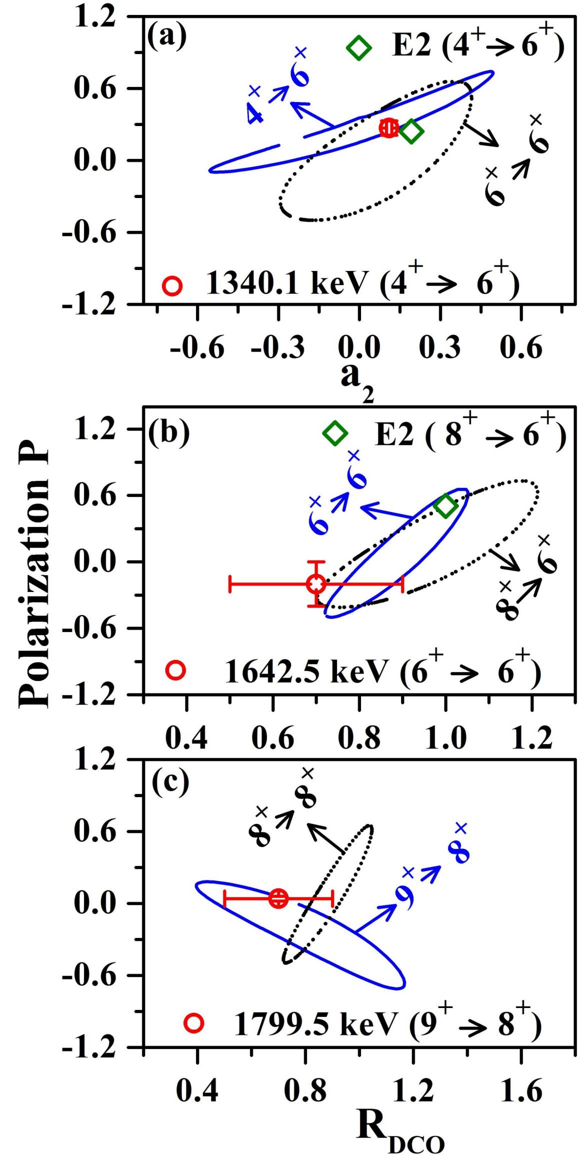

New candidate Tetrahedral sequence in ^{152}Sm

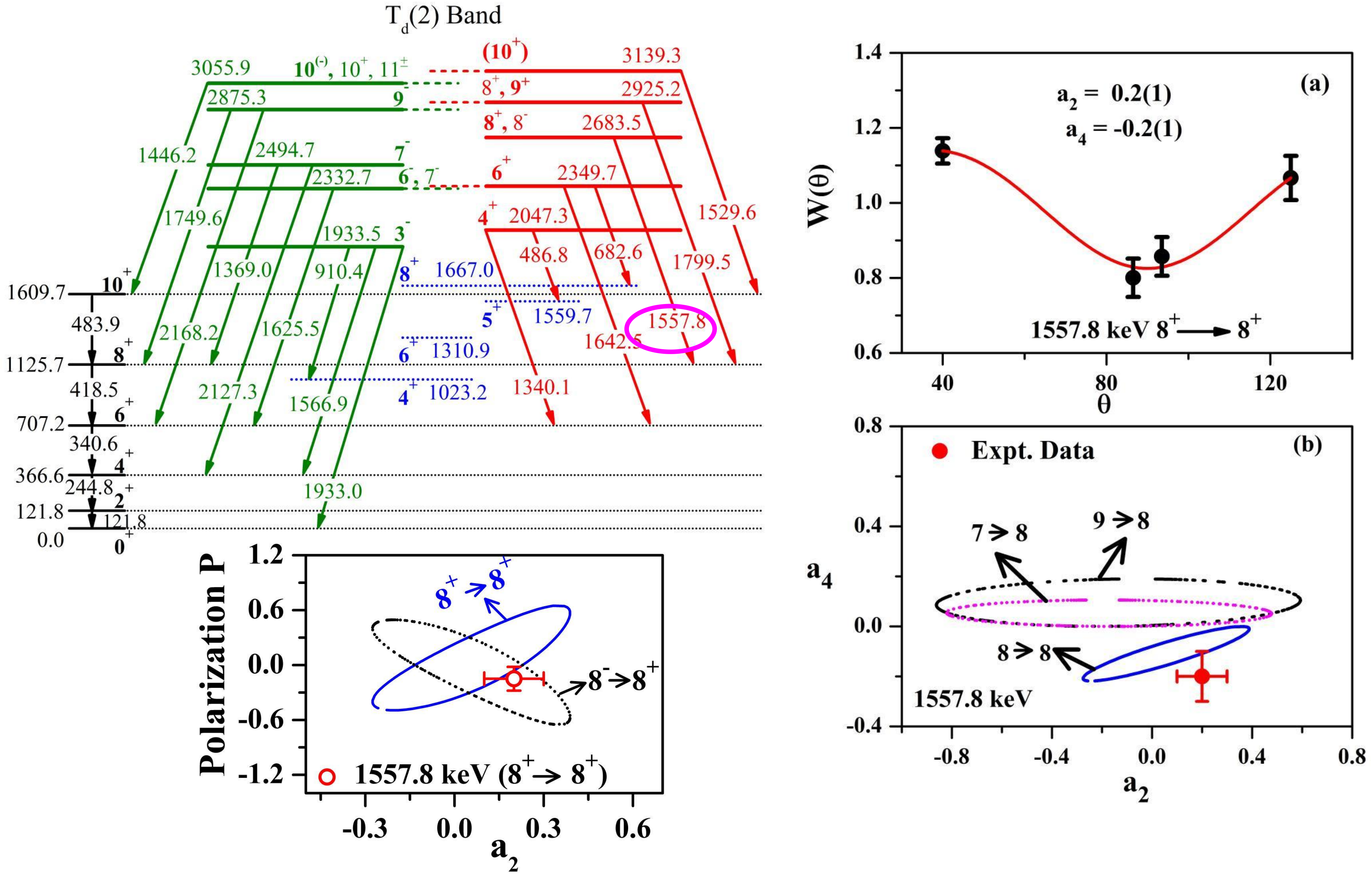

New candidate Tetrahedral sequence in ^{152}Sm

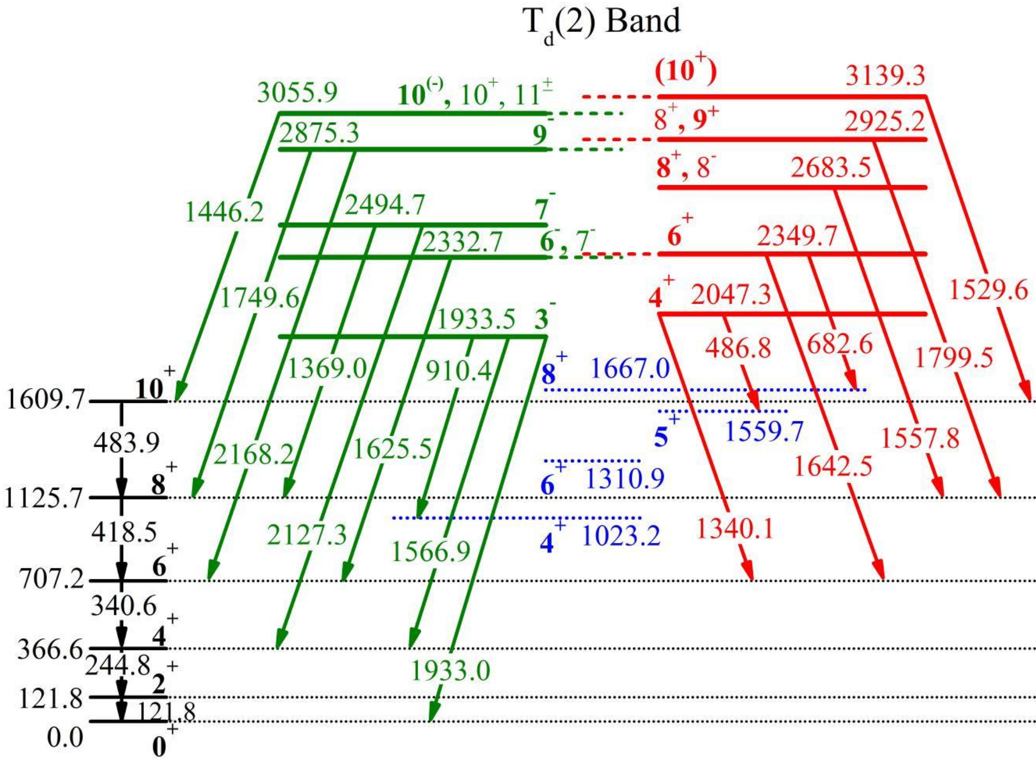

Level degeneracy

- Energies of 6^+, 6^- levels
- Energies of 9^+, 9^- levels
- Energies of 10^+, 10^- levels

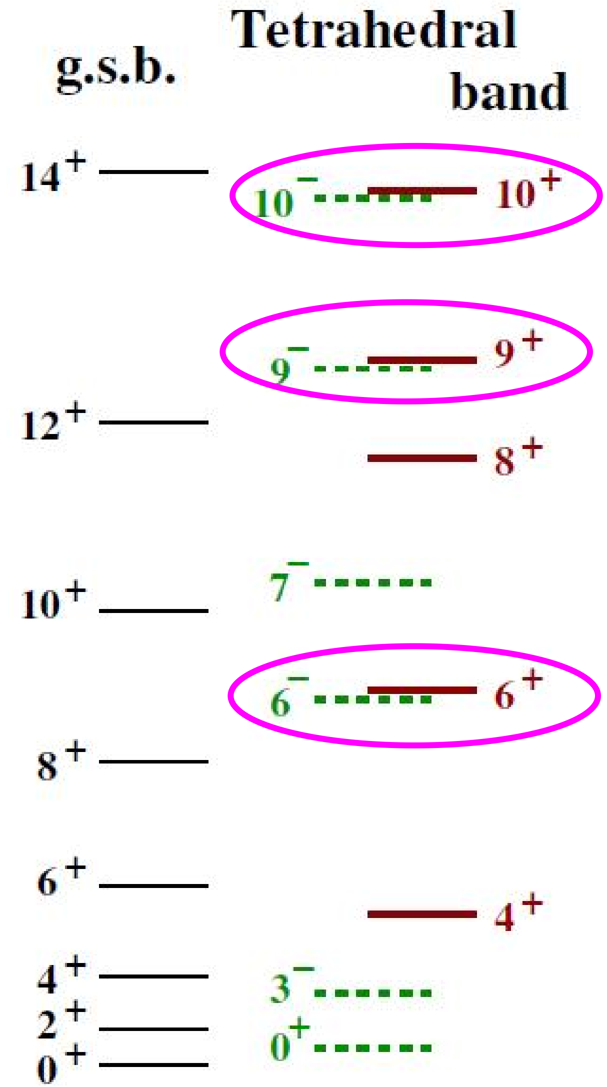

New candidate Tetrahedral sequence in ^{152}Sm

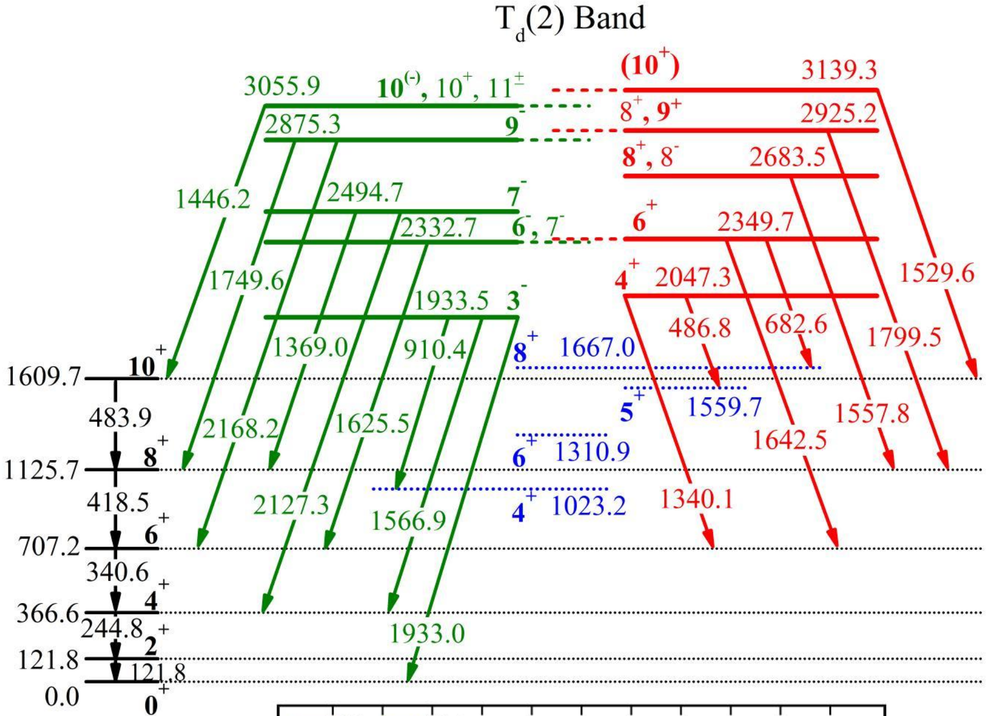

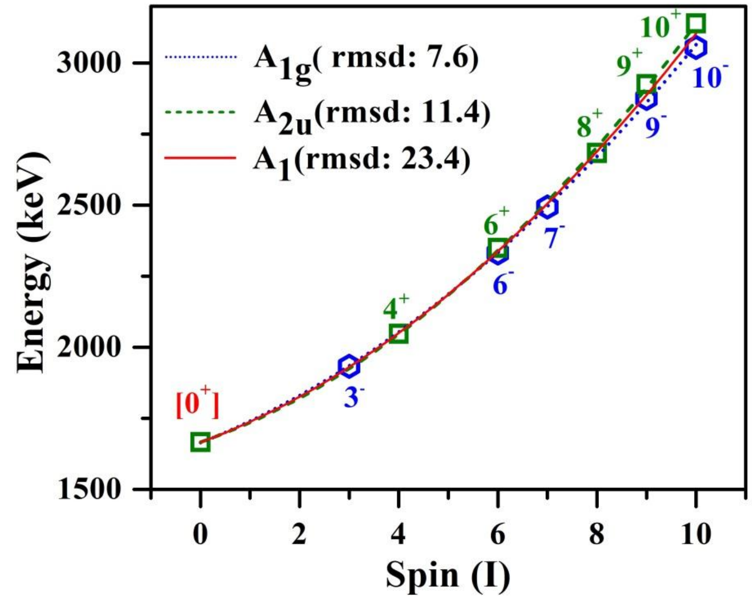

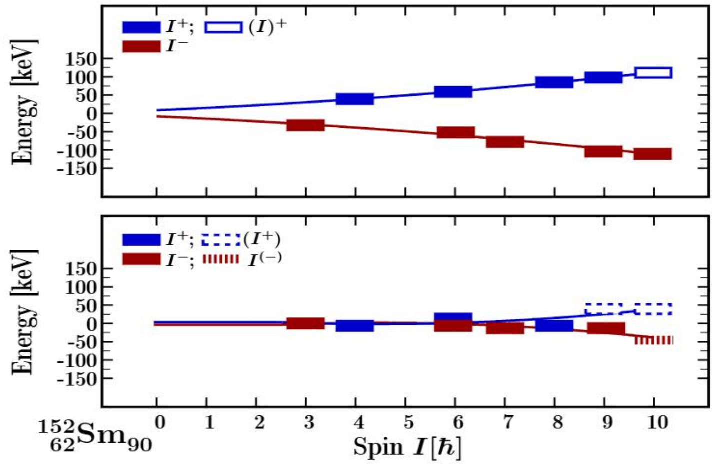

Experimental Results [T_d-*vs.*-O_h]

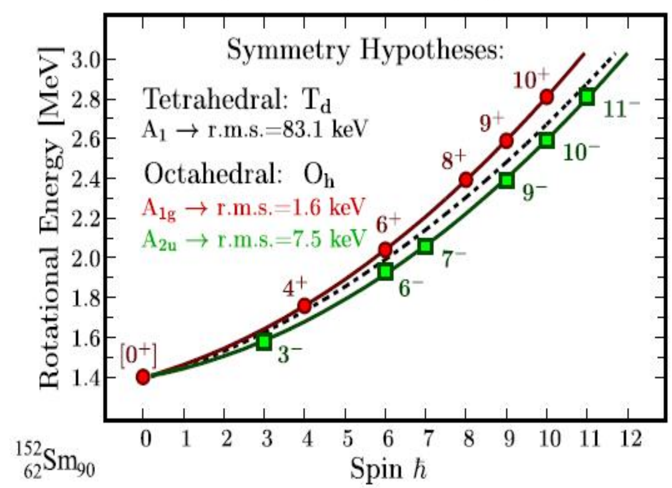

New candidate Tetrahedral sequence in ^{152}Sm

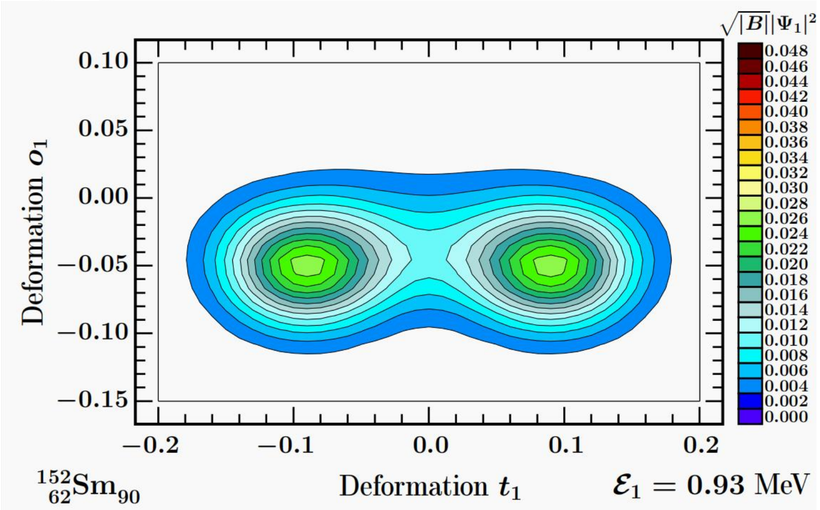

$$q_n^{dyn} \equiv \sqrt{\langle q_n^2 \rangle}, \quad t_1^{dyn} \approx 0.09 \text{ and } o_1^{dyn} \approx -0.04$$

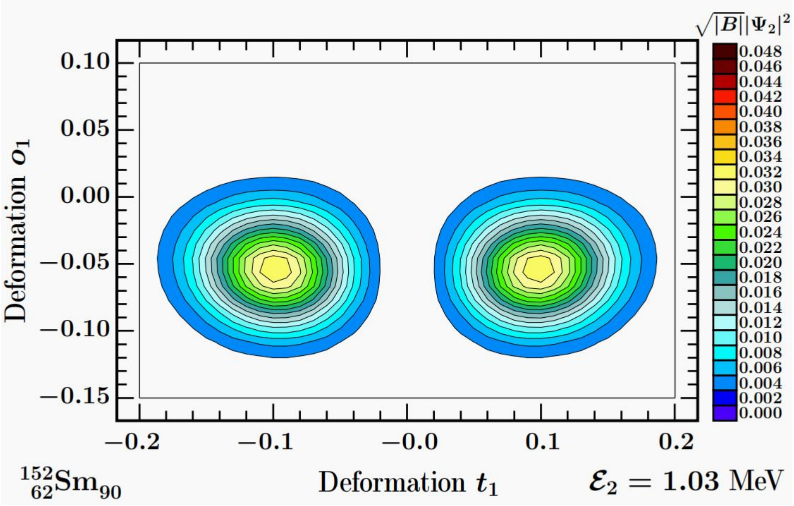

J. Dudek, I Dedes et al.,

$$\hat{H}\Psi_i = \mathcal{E}_i \Psi_i,$$

$$\hat{H} = -\frac{\hbar^2}{2}\hat{\Delta} + V(q),$$

$$\hat{\Delta} = \sum_{m,n=1}^{d=2} \frac{1}{\sqrt{|B|}} \frac{\partial}{\partial q^n}\left(\sqrt{|B|}B^{nm}\frac{\partial}{\partial q^m}\right),$$

- Probability density function for each of the solutions
- Quantum probability of finding the system within a deformation volume dV

$$d\mathcal{P}(q) \stackrel{df.}{=} \Psi_i^*(q)\Psi_i(q)\sqrt{|B|}\,dV, \quad dV \equiv dq_1 dq_2$$

$$\langle q_n^2 \rangle \stackrel{df.}{=} \int \Psi_i^*(q) q_n^2\, \Psi_i(q)\sqrt{|B|}\,dV, \quad dV \equiv dq_1 dq_2$$

New candidate Tetrahedral sequence in ^{152}Sm

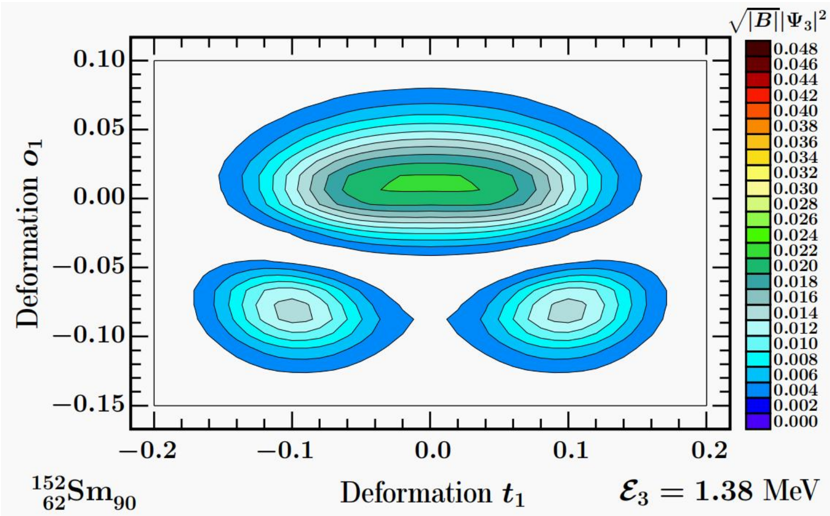

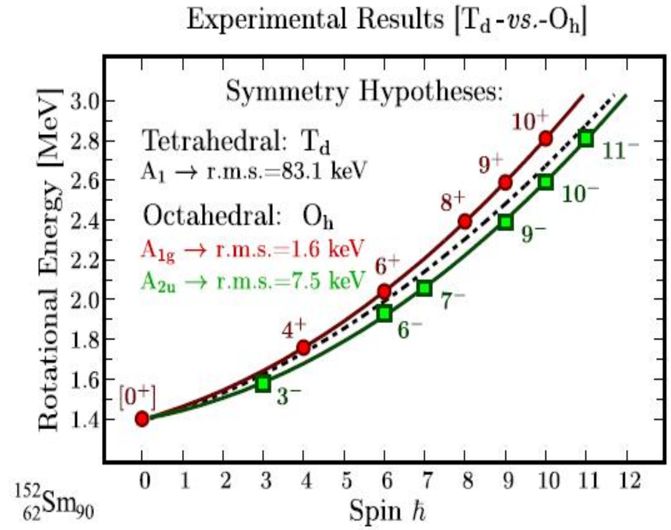

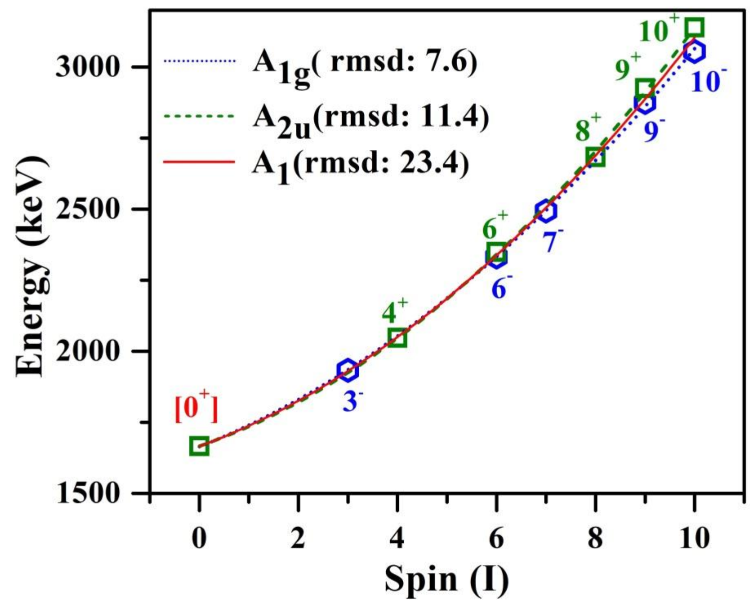

$$t_1^{\rm dyn} \approx 0.07 \ \text{ and } \ o_1^{\rm dyn} \approx 0$$

New candidate tetrahedral sequence is pure and preserve the octahedral symmetry

Summary

- ^{152}Sm : Rich example of shapes and shape co-existence
- The first tetrahedral candidate band was proposed in 2018
- Second tetrahedral candidate band is identified in the present work
- The new band shows the signature of pure tetrahedral structure retaining the octahedral symmetry
- Both the symmetry breaking compete in ^{152}Sm as found from the theoretical calculations

Collaborators

Devesh Kumar, Shefali Basak, Anandagopal Pal, Safikul alam, Arindam Kumar Sikdar, Joydip Nandi, Parnika Das

Abhijit Bisoi, sangeeta Das, Rozina Rahaman, Anik Adhikari, Arkadip Bera, Yajnya Sapkota, Ananya Das

Arunabha Saha

Saradindu Samanta, Suvronil Chatterjee, Rajarshi Raut, Sandeep S. Ghugre

Arnab Bhattacharyya, Priyabrato Das, Ushasi Datta

Manipal University Jaipur

Sathi Sharma

Jerzy Dudek, Gilbert Duchene, Dominique Curien

J. Yang

Irene Dedes, A. Gaamouci

Acknowledgement:

Dr. Sumit Som, Director, VECC, Kolkata

Prof. Jane Alam, Ex Head, Physics Group, VECC, Kolkata

Prof Sukalyan Chattopadhyay, Ex Head Physics Group, SINP, Kolkata

Dr. Sandip Ghugre, Director, UGC-DAE-CSR, Kolkata

Thank you for your attention!!

Shape Coexistence in ^{152}Sm

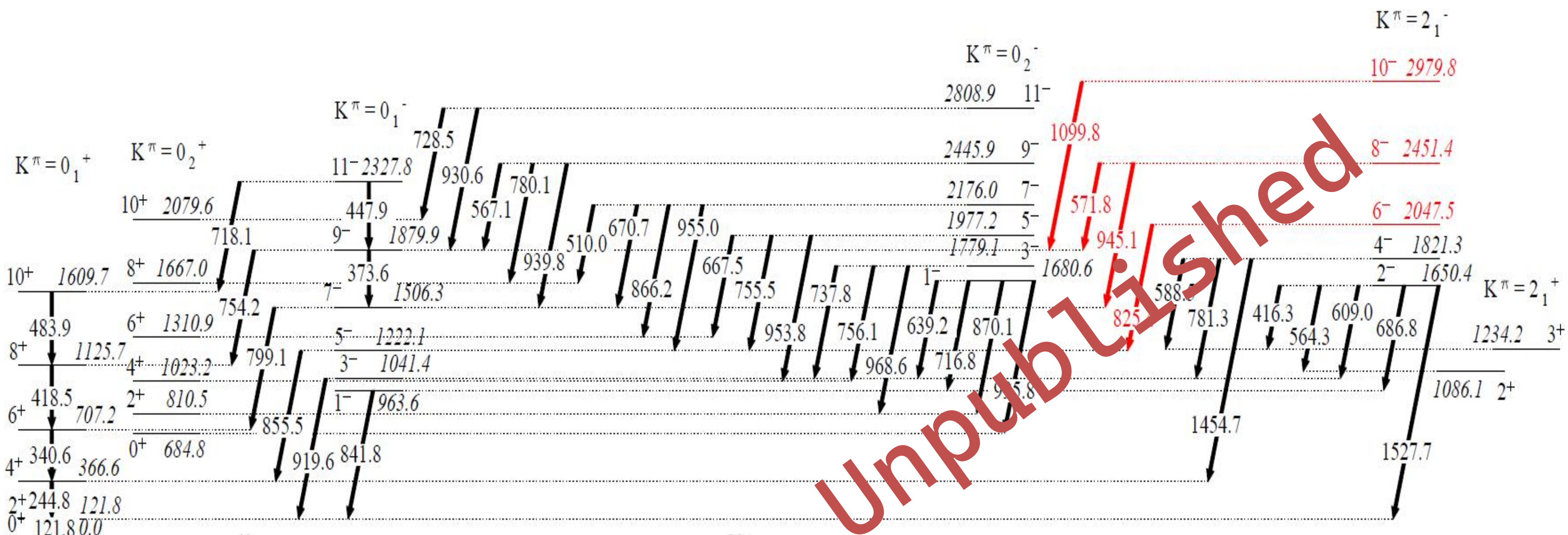

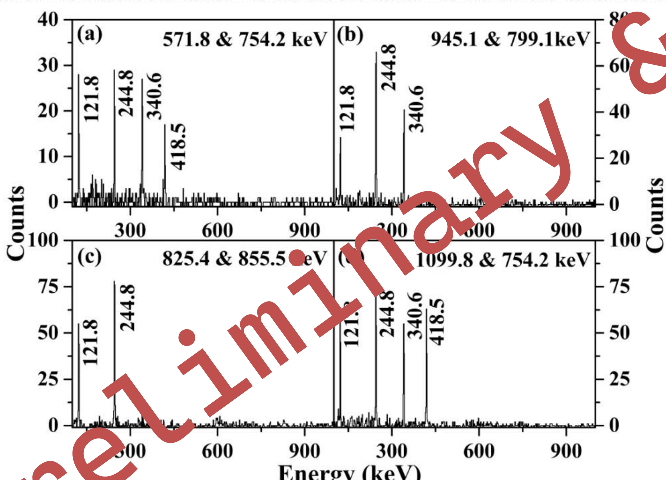

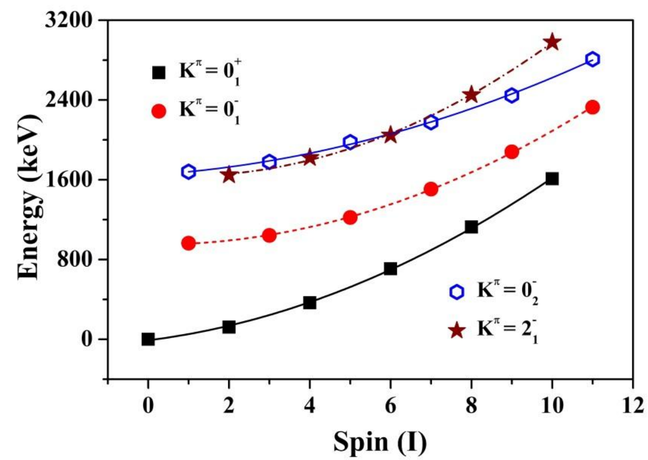

Competition between Tetrahedral and Octahedral Symmetries in ^{152}Sm Nucleus: A New set of data from a dedicated experiment	Tumpa Bhattacharjee, VECC, Kolkata	International Conference on Shapes and Symmetries in Nuclei – From Experiment to Theory (SSNET -2024) IJC Lab, France, November 04th – 08th, 2024

Shape Coexistence in ^{152}Sm

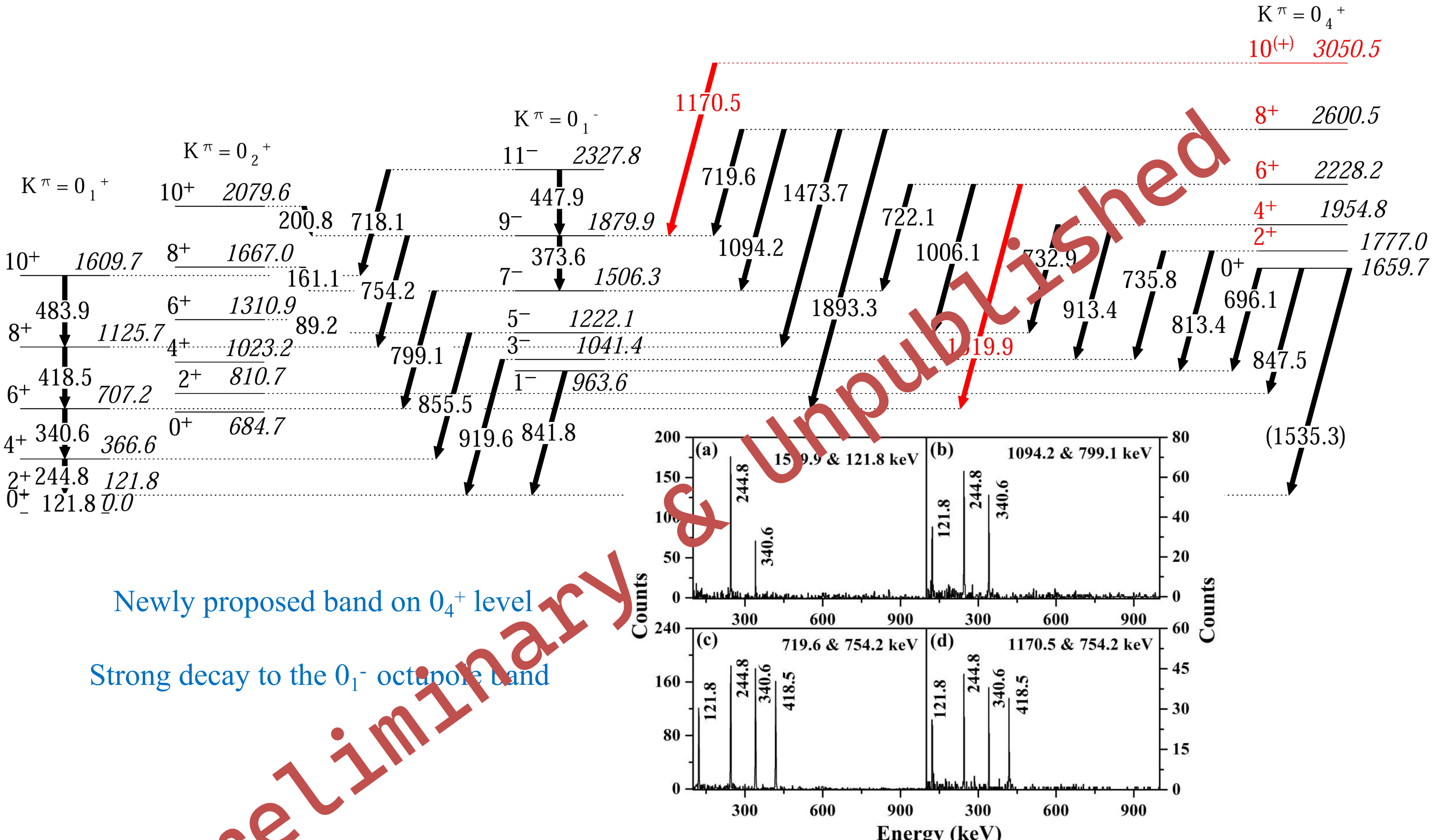

Newly proposed band on 0_4^+ level

Strong decay to the 0_1^- octupole band

Shape Coexistence in ^{152}Sm

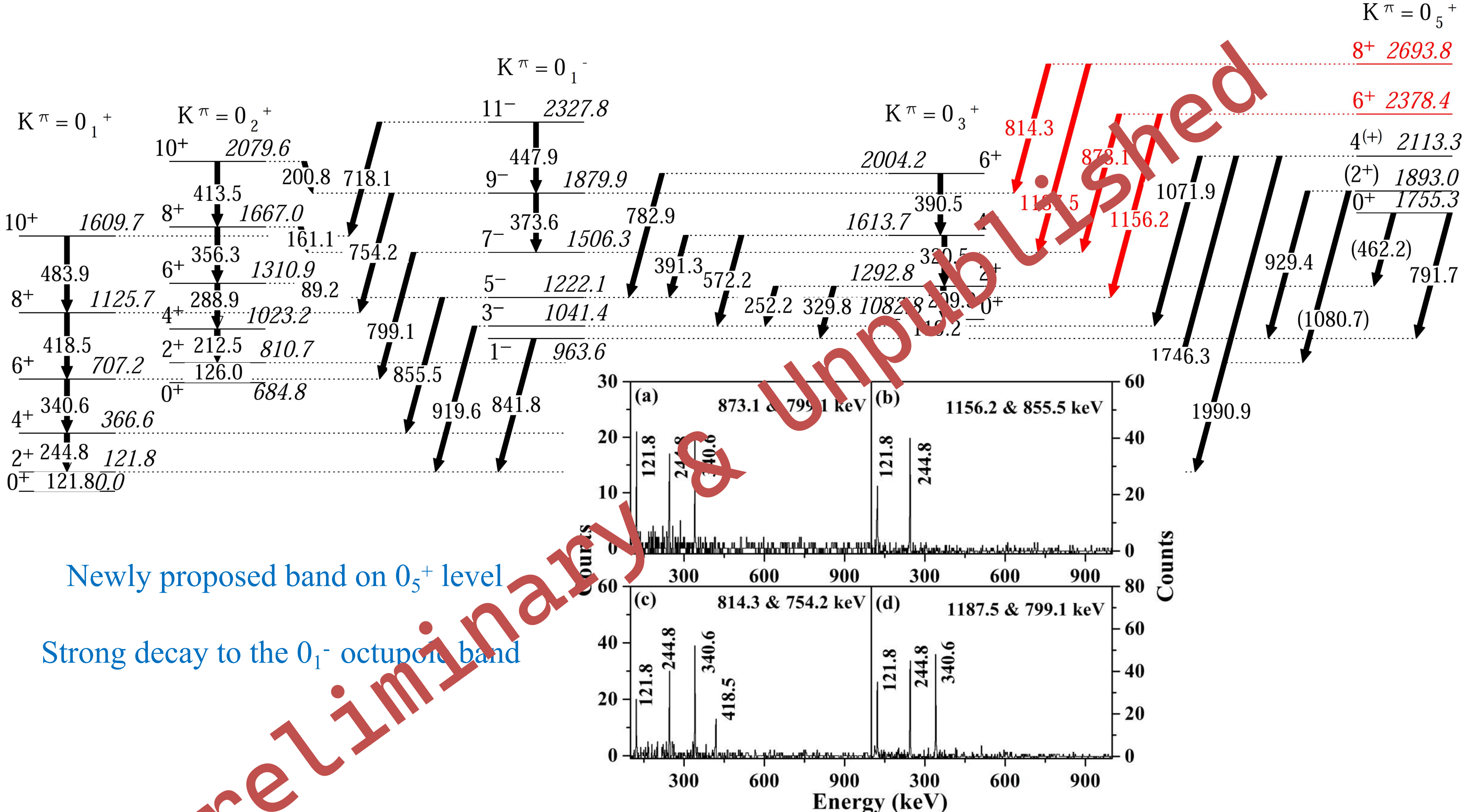

Newly proposed band on 0_5^+ level

Strong decay to the 0_1^- octupole band

Shape Coexistence in ^{152}Sm

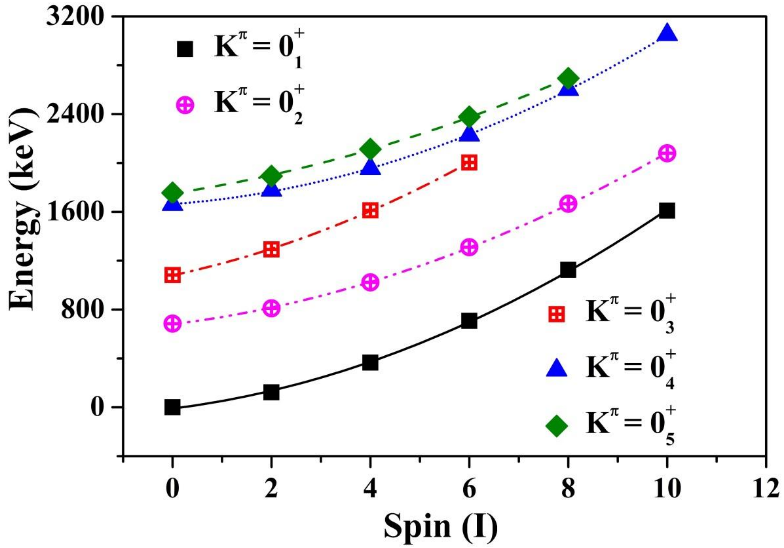

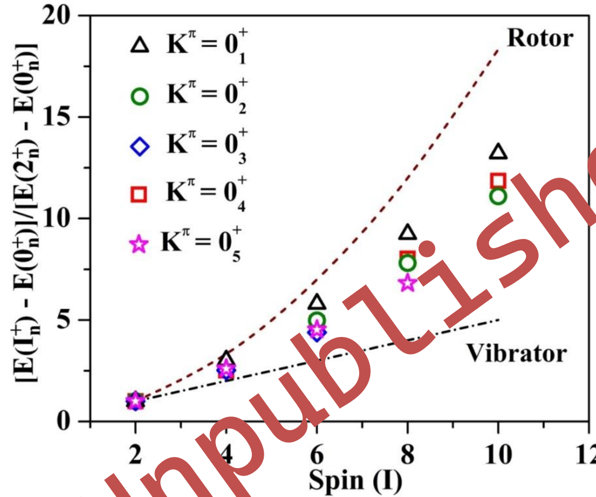

(X5 symmetry)

N = 90 ^{152}Sm displays all of quadrupole – quadrupole, quadrupole – octupole, octupole – octupole shape co-existence

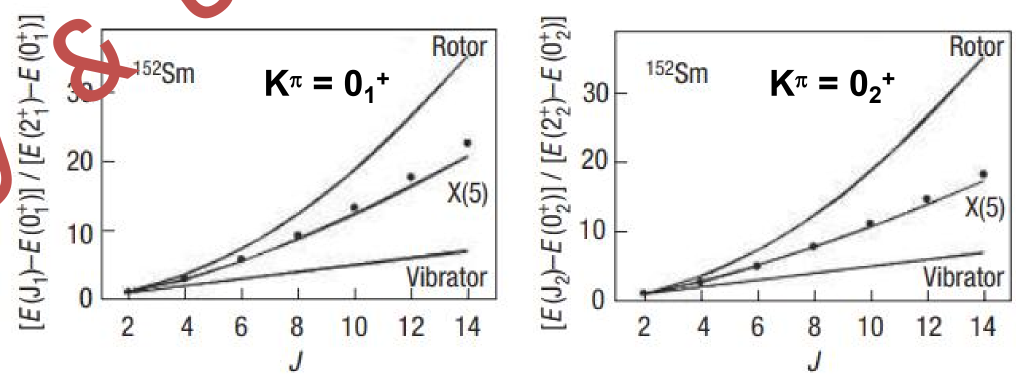

R.F. Casten, Nature Physics 2, 811 (2006)

γ–γ Matrix & γ–γ–γ cube – Development of level scheme

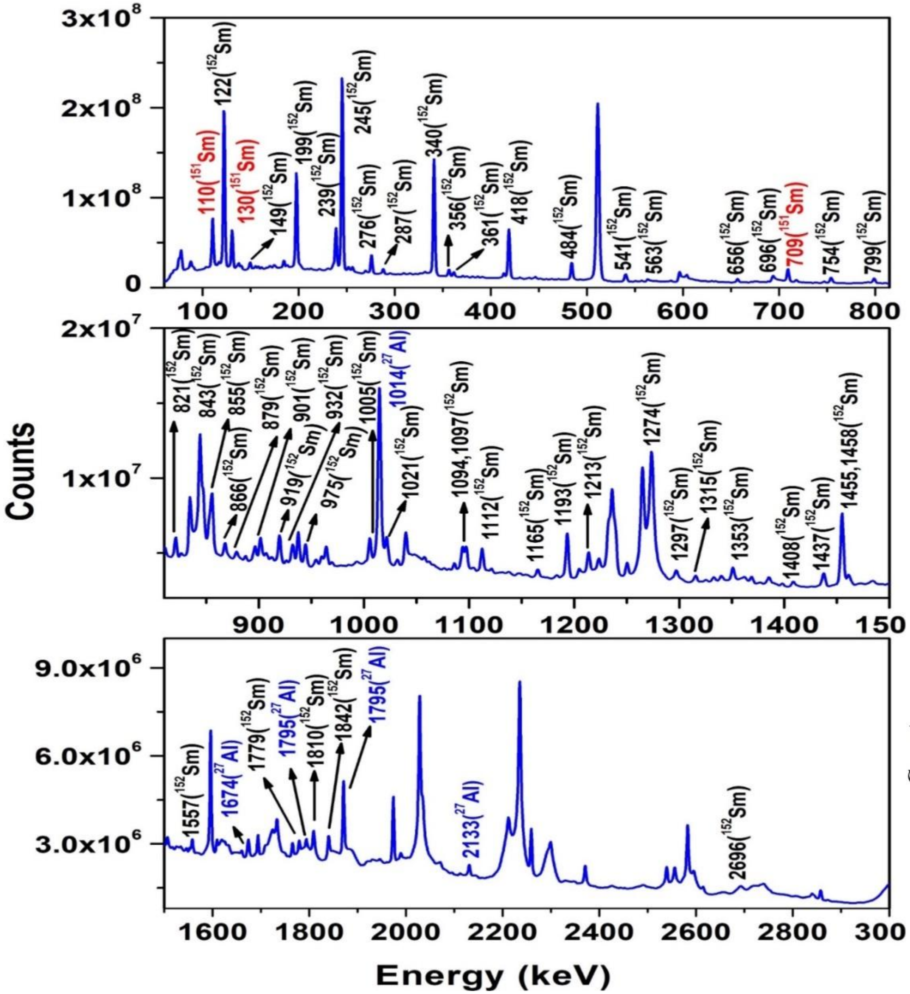

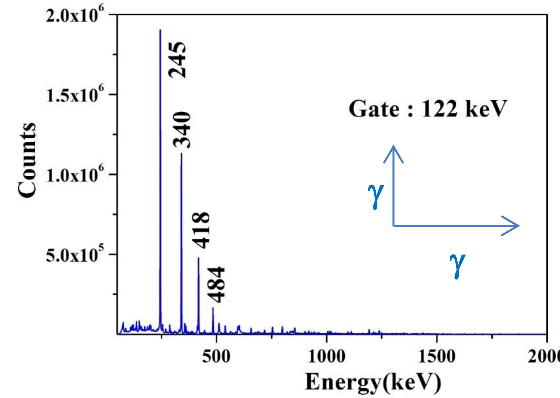

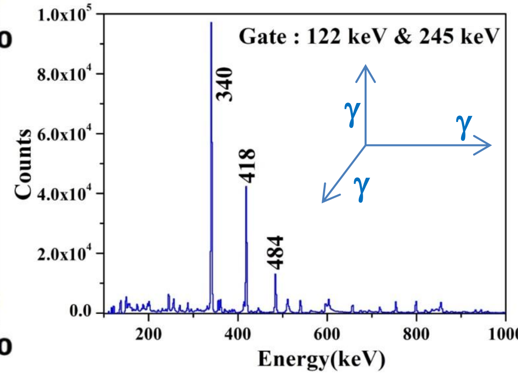

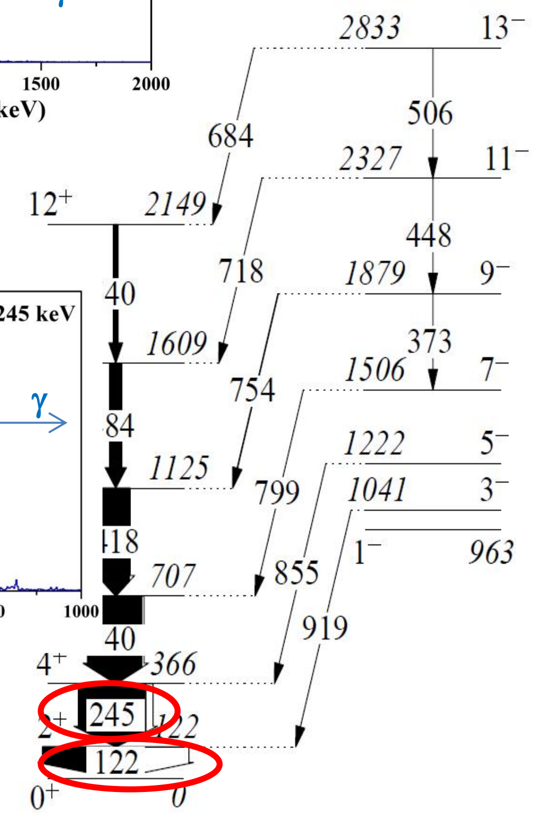

Angular Distribution measurement for determination of Multipolarity

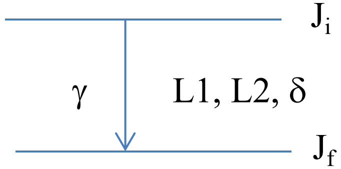

$$W(\theta) = A_0 + A_2P_2(cos\theta) + A_4P_4(cos\theta) = A_0[1 + a_2P_2(cos\theta) + a_4P_4(cos\theta)]$$

- θ: 40^0, 86.5^0, 93.5^0, 125^0
- 86.5^0 and 93.5^0 → from 90^0 clovers opening angle of the Clover as 7^0

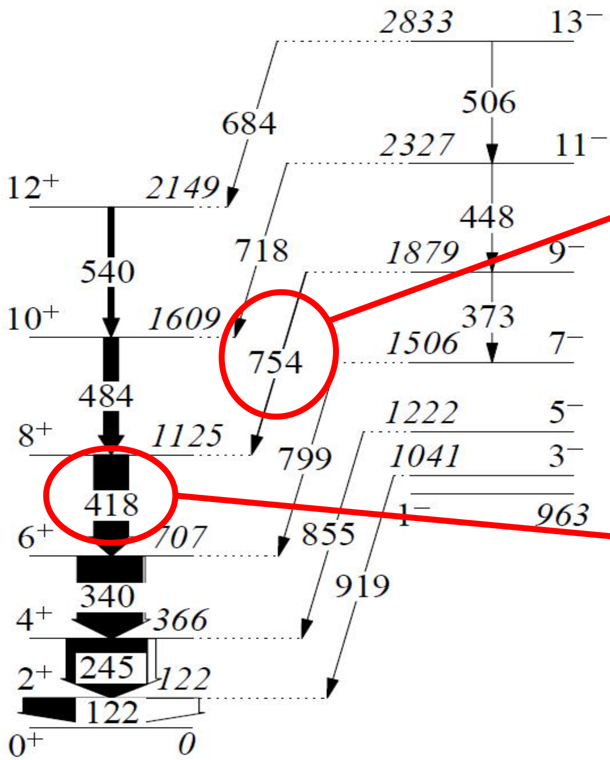

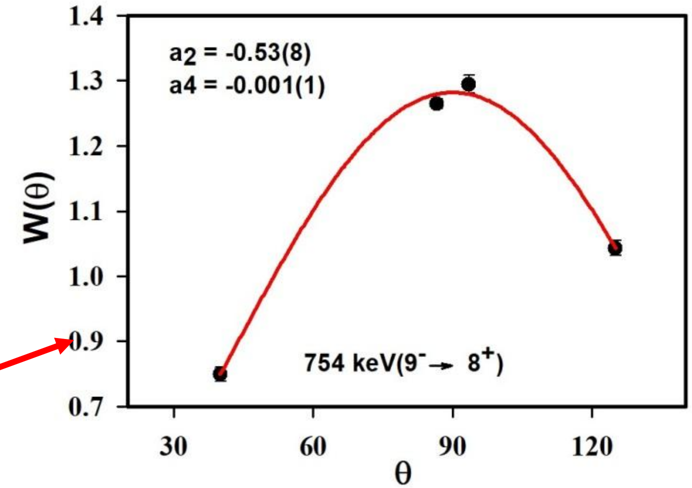

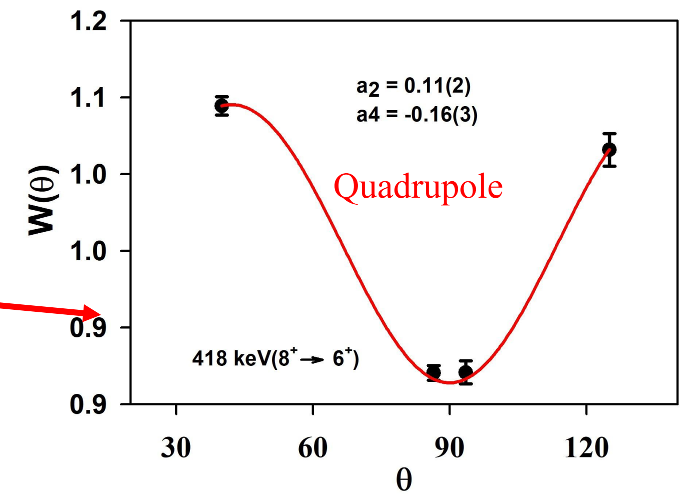

DCO Ratio for determination of Multipolarity

$$\mathrm{DCO}(\gamma_1) = \frac{I_{\gamma_1}(125^\circ),\ \text{gated by } \gamma_2 \text{ at } 90^\circ}{I_{\gamma_1}(90^\circ),\ \text{gated by } \gamma_2 \text{ at } 125^\circ}$$

For 418 keV transition (E2) : R_{DCO} = 0.98(2) in Quadrupole gate

For 799 keV transition (E1) : R_{DCO} = 0.67(1) in Quadrupole gate

For 251 keV transition (E1) : R_{DCO} = 1.1(1) in Dipole gate

For 446 keV transition (E2) : R_{DCO} = 1.6(2) in Dipole gate

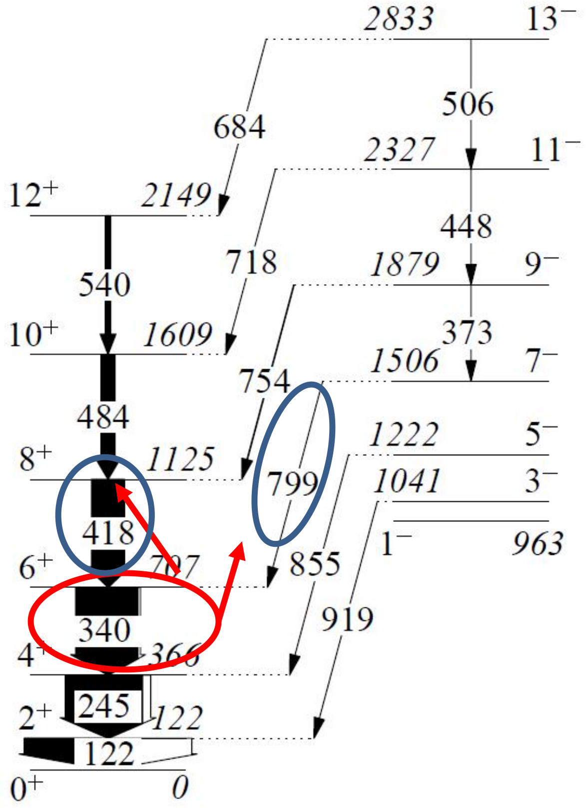

Linear Polarization - Determination of Parity

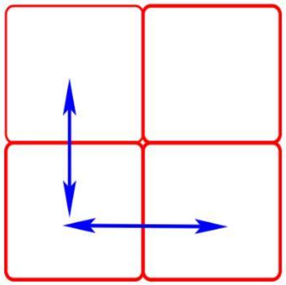

Experimental Method of Linear Polarization Measurement

$$P(\theta) = \frac{IPDCO}{Q(E_\gamma)} \qquad Q(E_\gamma) = Q_0(a + b \times E_\gamma),$$

$$Q_0 = \frac{(1+\alpha)}{(1+\alpha+\alpha^2)} \quad \text{with } \alpha = \frac{E_\gamma\ (\text{keV})}{511}$$

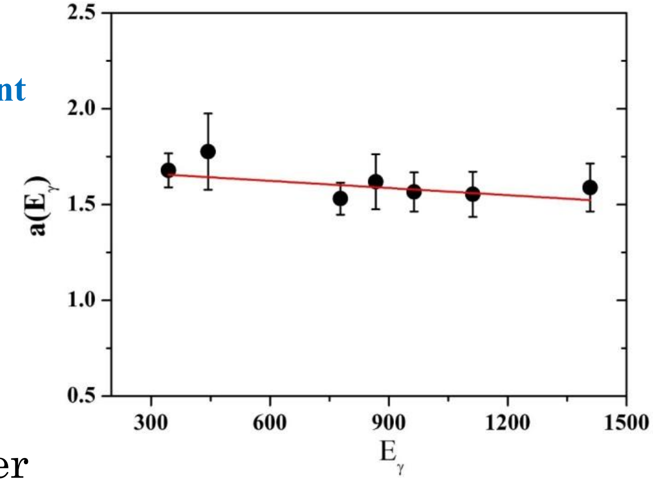

Q_0 = polarization sensitivity for the ideal Compton polarimeter

$$IPDCO = \frac{a(E_\gamma)N_\perp - N_\parallel}{a(E_\gamma)N_\perp + N_\parallel} \qquad a(E_\gamma) = \frac{N_\parallel}{N_\perp}$$

- +ve → Electric Transition
- -ve → Magnetic Transition
- 0 → Mixed Transition

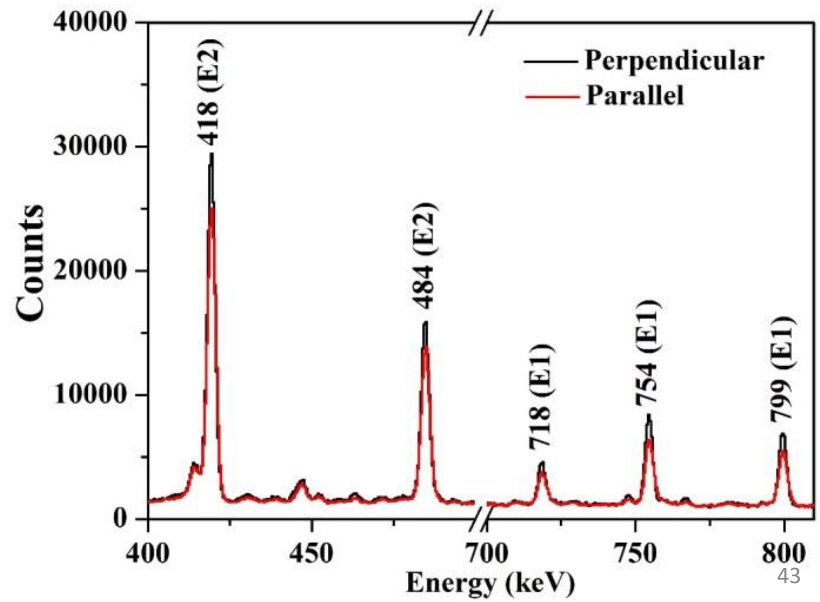

R_{DCO} & IPDCO values in ^{152}Sm

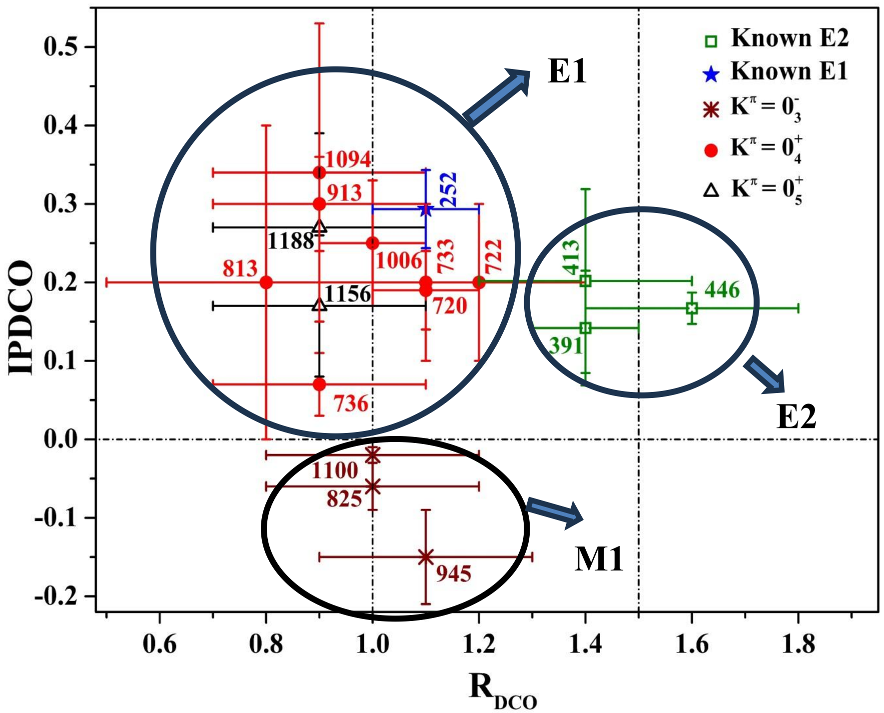

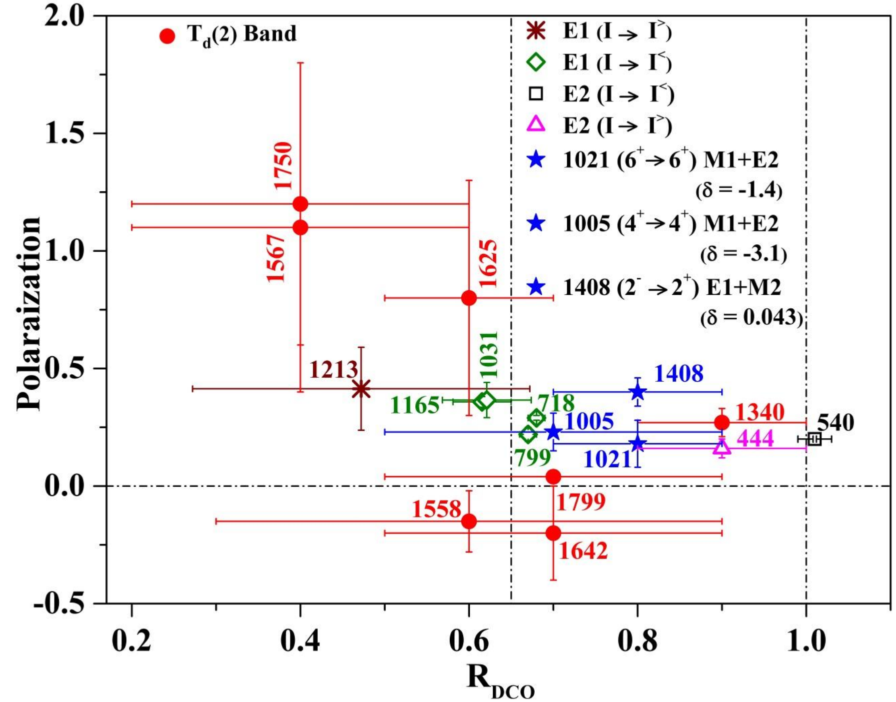

Calculation of angular distribution coefficients, DCO Ratio and Polarization

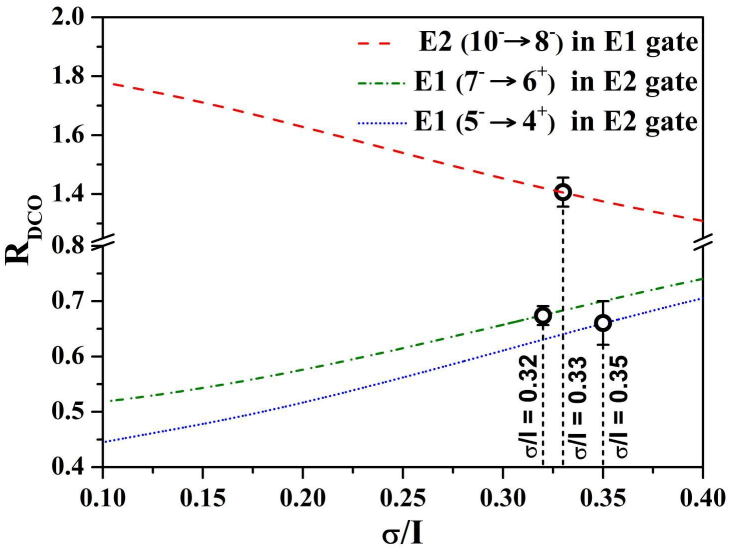

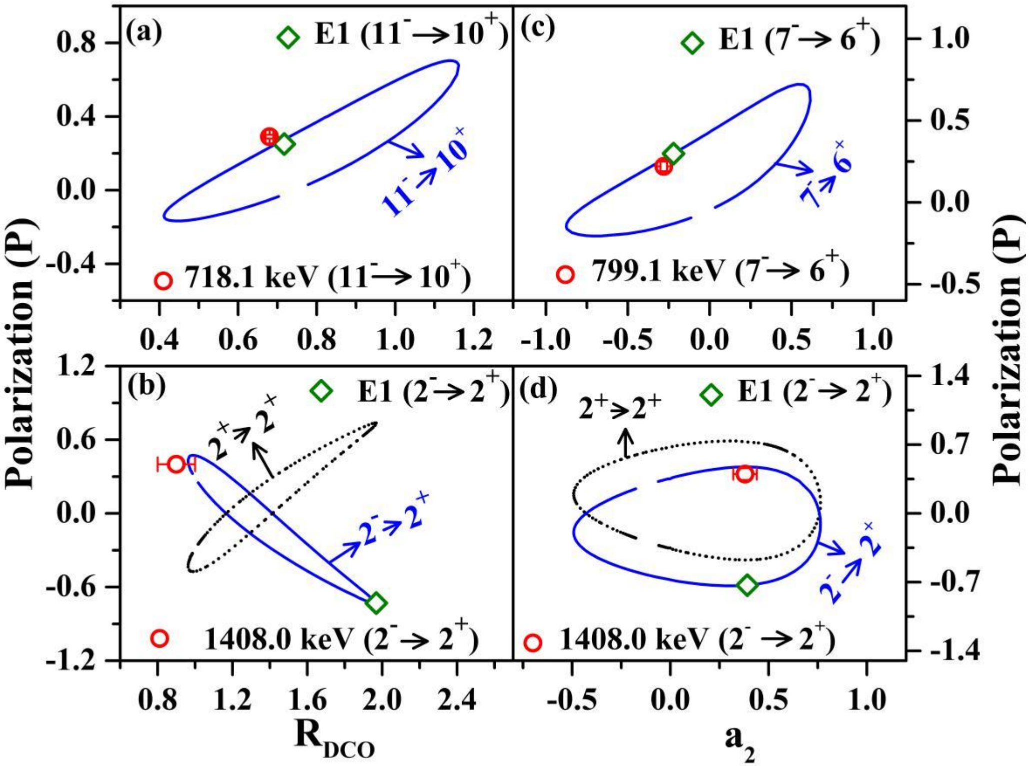

σ/J = 0.33

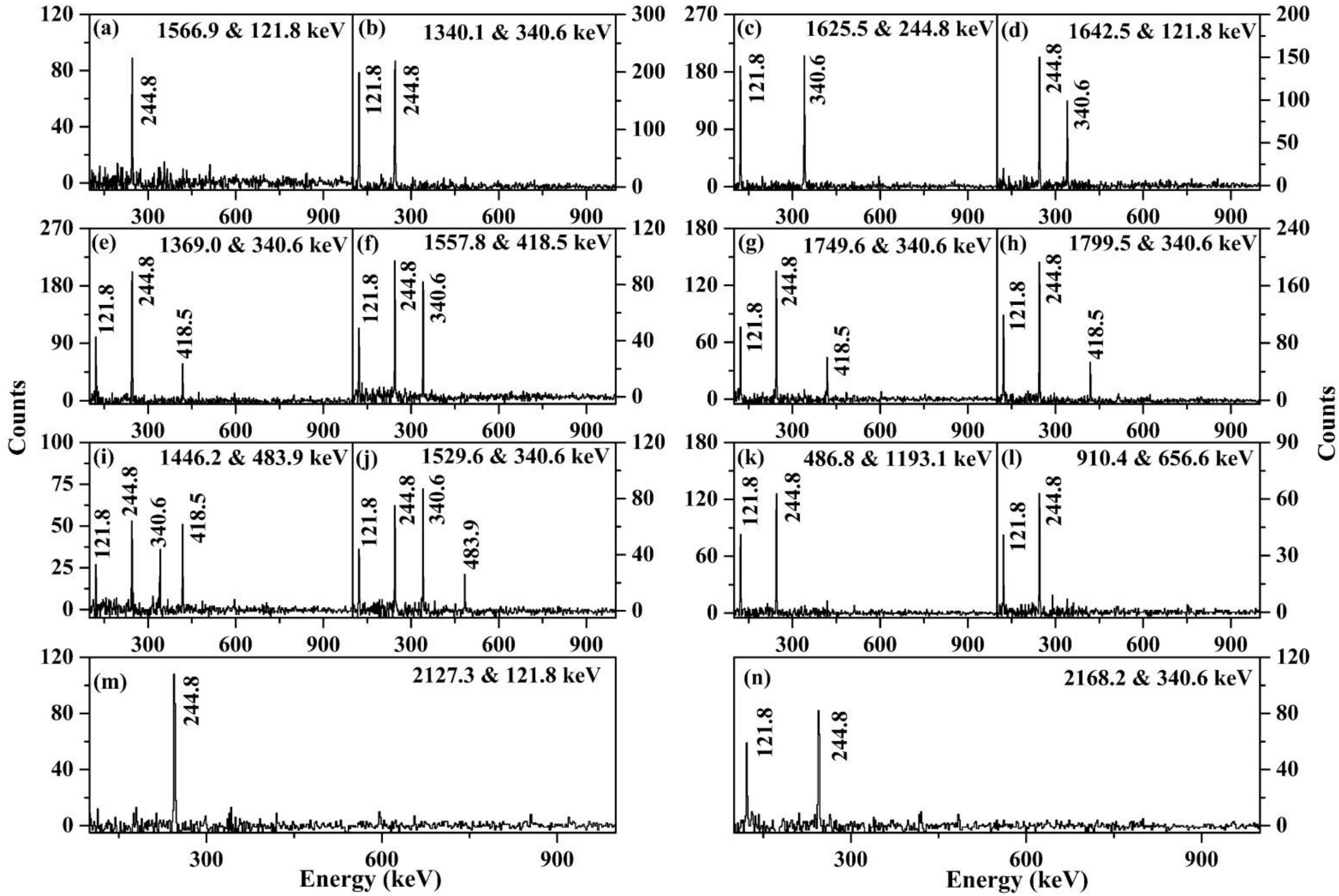

(a) 1566.9 & 121.8 keV
244.8
(b) 1340.1 & 340.6 keV
121.8
244.8
(c) 1625.5 & 244.8 keV
121.8
340.6
(d) 1642.5 & 121.8 keV
244.8
340.6
(e) 1369.0 & 340.6 keV
121.8
244.8
418.5
(f) 1557.8 & 418.5 keV
121.8
244.8
340.6
(g) 1749.6 & 340.6 keV
121.8
244.8
418.5
(h) 1799.5 & 340.6 keV
121.8
244.8
418.5
(i) 1446.2 & 483.9 keV
121.8
244.8
340.6
418.5
(j) 1529.6 & 340.6 keV
121.8
244.8
340.6
483.9
(k) 486.8 & 1193.1 keV
121.8
244.8
(l) 910.4 & 656.6 keV
121.8
244.8
(m) 2127.3 & 121.8 keV
244.8
(n) 2168.2 & 340.6 keV
121.8
244.8
Counts
Energy (keV)

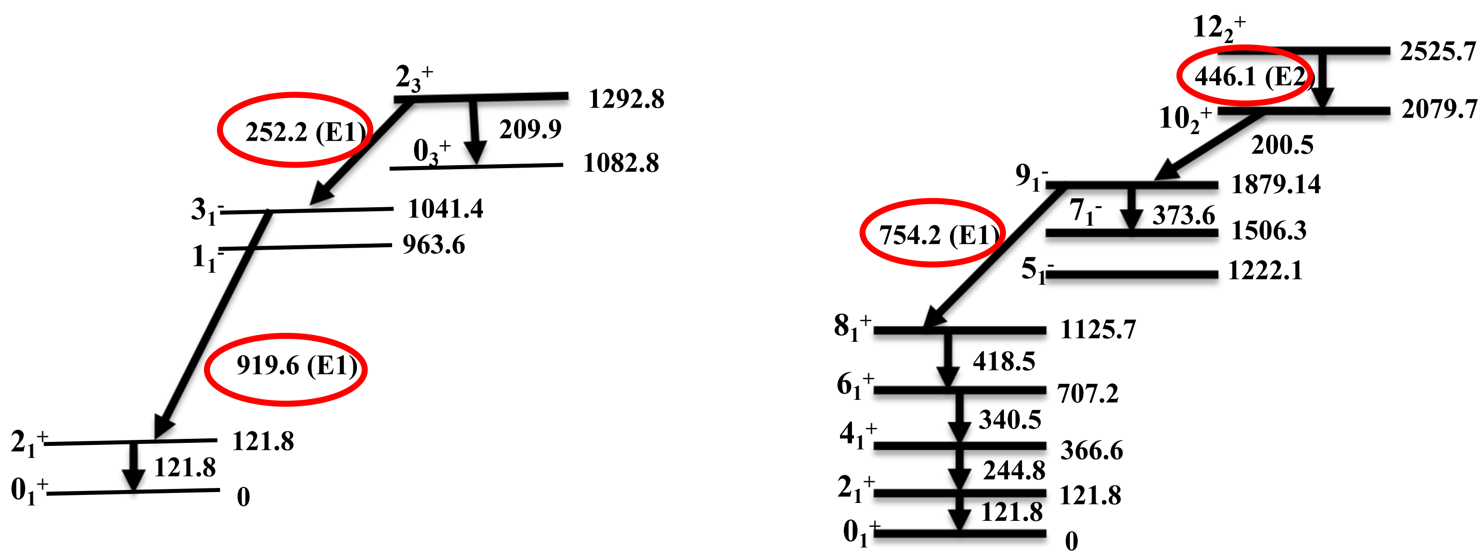

2_3^+
1292.8
252.2 (E1)
209.9
0_3^+
1082.8
3_1^-
1041.4
1_1^-
963.6
919.6 (E1)
2_1^+
121.8
121.8
0_1^+
0
12_2^+
2525.7
446.1 (E2)
10_2^+
2079.7
200.5
9_1^-
1879.14
7_1^-
373.6
1506.3
754.2 (E1)
5_1^-
1222.1
8_1^+
1125.7
418.5
6_1^+
707.2
340.5
4_1^+
366.6
244.8
2_1^+
121.8
121.8
0_1^+
0

Thank You

Array Configuration

$$P(\theta) = (\pm)\frac{\sum_{\nu} a_{\nu}\kappa(l,l')P_{\nu}^{2}(cos\theta)}{1+\sum_{\nu} a_{\nu}P_{\nu}(cos\theta)}.$$

A. Pal et al, Unpublished, under review.

Nuclear Structure @ Tetrahedral Shape

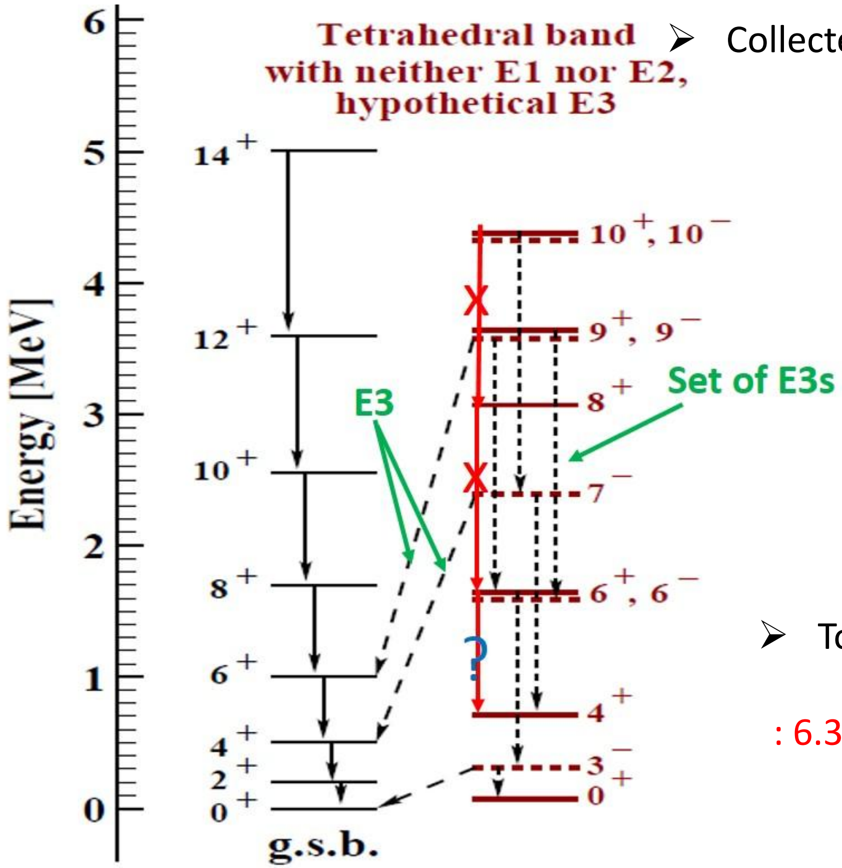

- Collected data in singles mode (remarkable performance by the Digital DAQ)

- Number of Clovers with 4 crystals working: 6
- Number of Clovers with 4 crystals working: 4
  - Total number of working crystals: 39
- Total beam time (BOT) consumed : 11.5 days

- Total γ–γ events gathered (good data from 60 keV - 2 MeV)
  : 2.2 x 10^9 γ–γ events (with background) → ^{152}Sm
  : 6.3 x 10^8 γ–γ events (after background subtraction) → ^{152}Sm
  :8.4 x 10^7 events under 2^+ → 0^+ peak (121 keV)

Gain drift → 80 sets of list files to be sorted → 76 matrices with pixisort [S. Das et al., NIMA **893**, 138(2018)] that were added to generate the matrix